Supplemental Material can be found at:
http://www.jbc.org/content/suppl/2010/01/10/M109.053348.DC1.html

THE JOURNAL OF BIOLOGICAL CHEMISTRY VOL. 285, NO. 14, pp. 10761–10776, April 2, 2010
© 2010 by The American Society for Biochemistry and Molecular Biology, Inc. Printed in the U.S.A.

E-cadherin Differentially Regulates the Assembly of Connexin43 and Connexin32 into Gap Junctions in Human Squamous Carcinoma Cells*[S]

Received for publication, August 8, 2009, and in revised form, December 31, 2009 Published, JBC Papers in Press, January 19, 2010, DOI 10.1074/jbc.M109.053348

Souvik Chakraborty[‡], Shalini Mitra[‡], Matthias M. Falk[§], Steve H. Caplan[‡], Margaret J. Wheelock[‡], Keith R. Johnson[‡], and Parmender P. Mehta[‡1]

From the [‡]Department of Biochemistry and Molecular Biology, Eppley Institute for Research in Cancer and Allied Diseases, Eppley Cancer Center, University of Nebraska Medical Center, Omaha, Nebraska 68198 and the [§]Department of Biological Sciences, Lehigh University, Bethlehem, Pennsylvania 18015

It is as yet unknown how the assembly of connexins (Cx) into gap junctions (GJ) is initiated upon cell-cell contact. We investigated whether the trafficking and assembly of Cx43 and Cx32 into GJs were contingent upon cell-cell adhesion mediated by E-cadherin. We also examined the role of the carboxyl termini of these Cxs in initiating the formation of GJs. Using cadherin and Cx-null cells, and by introducing Cx43 and Cx32, either alone or in combination with E-cadherin, our studies demonstrated that E-cadherin-mediated cell-cell adhesion was neither essential nor sufficient to initiate GJ assembly *de novo* in A431D human squamous carcinoma cells. However, E-cadherin facilitated the growth and assembly of preformed GJs composed of Cx43, although the growth of cells on Transwell filters was required to initiate the assembly of Cx32. Our results also documented that the carboxyl termini of both Cxs were required in this cell type to initiate the formation of GJs *de novo*. Our findings also showed that GJ puncta composed of Cx43 co-localized extensively with ZO-1 and actin fibers at cell peripheries and that ZO-1 knockdown attenuated Cx43 assembly. These findings suggest that the assembly of Cx43 and Cx32 into GJs is differentially modulated by E-cadherin-mediated cell-cell adhesion and that direct or indirect cross-talk between carboxyl tails of Cxs and actin cytoskeleton via ZO-1 may regulate GJ assembly and growth.

Gap junctions are conglomerations of intercellular channels that permit the direct exchange of ions, second messengers, and other molecules of less than 1500 Da between the cytoplasmic interiors of contiguous cells. The channels are composed of a family of proteins called connexins (Cx)[2] that are designated according to their molecular mass (1). The assembly of Cxs into GJs is a multistep process. The newly synthesized Cxs are co-translationally inserted into the endoplasmic reticulum, which oligomerize to form hexamers called connexons. The connexons are delivered to the cell surface via Golgi and trans-Golgi network in small vesicles and dock with the connexons in the contiguous cell membranes to form intercellular channels. A GJ plaque is formed when several intercellular channels cluster (2, 3). Because of the short half-life of Cxs (2–5 h), the plaque is in a dynamic state and is thought to model and remodel constantly through recruitment of newly synthesized connexons to the periphery and through endocytosis of moribund plaque components from the center or through the endocytosis of the plaque in its entirety (4–7). Although much has been learned about the intracellular transport of Cxs, the delivery of connexons to the cell surface, the formation of cell-to-cell channels, the spatio-temporal events and cellular factors required for the initial docking of connexons, the *de novo* formation of a nascent GJ plaque, its growth, and disassembly are poorly understood (2, 8).

The proximity between the plasma membranes of adjoining cells is, *a priori*, necessary for the formation of GJs, and cell-cell adhesion has been thought to facilitate this process. Cell-cell adhesion is mediated by cadherins, which belong to a large family of transmembrane proteins. Of all the cadherins, the most predominant isoform expressed in epithelial cells is the epithelial (E)-cadherin (9–11). Apart from controlling the formation of tight junctions and desmosomes, forced expression of E-cadherin has been shown to restore cell-cell adhesion and induce GJ assembly, and abolition of cadherin mediated cell-cell adhesion has been shown to disrupt the assembly (12–15). Despite these studies, the possible mechanism(s) by which cadherins might regulate GJ assembly have yet to be explored. The importance of undertaking these studies is underscored by the fact that dysfunctional E-cadherin-mediated cell-cell adhesion as well as aberrant assembly of Cxs into GJs are the hallmarks of cancer progression (16–18).

Here we sought to investigate if cell-cell adhesion mediated by E-cadherin expression was sufficient by itself to induce the assembly of Cxs into GJs or whether additional events were required. Because both cadherins and Cxs belong to a large family of related proteins, and most cells *in vivo* and *in vitro* are likely to express more than one family member (2, 10, 18), we thought to delineate these mechanisms in a cell culture model

* This work was supported, in whole or in part, by National Institutes of Health Grants RO-1 CA113903 (to P. P. M.), RO-1DE12308 (to K. R. J.), and RO-1GM074876 (to S. H. C.). This work was also supported by Department of Defense Grant PC081198 and Nebraska State Grant LB506 (to P. P. M.) and the Nebraska Center for Cellular Signaling graduate fellowship (to S. M. and S. C.).

[S] The on-line version of this article (available at http://www.jbc.org) contains supplemental Figs. S1–S12.

[1] To whom correspondence should be addressed. Tel.: 402-559-3826; Fax: 402-559-6650; E-mail: pmehta@unmc.edu.

[2] The abbreviations used are: Cx, connexin; GJ, gap junction; PBS, phosphate-buffered saline; EYFP, enhanced yellow fluorescent protein; siRNA, small interfering RNA.

Downloaded from www.jbc.org at Lehigh University, on November 10, 2010

system that was Cx- and cadherin-null and where cadherins and Cxs could be introduced either alone or in combination (19, 20). Moreover, we rationalized that if the expression of a cadherin or cell-cell adhesion mediated by it *per se* was the sole determinant of the assembly of Cxs into GJs, then the assembly should be independent of the subtype of Cx introduced. Furthermore, because some Cxs are expressed in a tissue-specific manner (18), and have divergent carboxyl termini that might interact with the cadherins directly or indirectly to regulate GJ assembly (2, 18, 21, 22), we also assessed the role of these termini in initiating the formation of GJs in the presence and absence of E-cadherin.

Using cadherin- and Cx-null A431D cells, derived from human squamous carcinoma cell line A431(19, 20), and by introducing Cx43, a ubiquitously expressed Cx (22), and Cx32, a Cx preferentially expressed by the well differentiated and polarized cells (23), either alone or in combination with E-cadherin, we show that E-cadherin-mediated cell-cell adhesion facilitates the growth and assembly of only preformed GJs but is not sufficient to trigger the assembly of GJs *de novo*. We also show that in this cell system the carboxyl termini of Cx32 and Cx43 are required to initiate the formation of GJs *de novo*. Finally, our findings suggest a role for ZO-1 and actin filaments in initiating the formation or stabilization of GJs. Our data imply that the assembly of different Cxs into GJs is governed in a complex manner by E-cadherin, which in turn may depend on the motifs in the Cxs themselves and additional proteins that permit or impede docking of connexons and clustering of gap junctional channels.

MATERIALS AND METHODS

Cell Culture—The characterization of cadherin-null A431D and its E-cadherin-expressing counterpart, A431DE, has been described (19). These cells were grown in Dulbecco's modified Eagle's medium (Invitrogen) supplemented with 2.5% defined fetal bovine serum and 2.5% bovine growth serum (Hyclone, Salt Lake City, UT) in an atmosphere of 5% CO_2, 95% air. A431DE cells were maintained in complete medium containing puromycin (2 μg/ml). Connexin-expressing A431D and A431DE clones were isolated as described (see under "Retrovirus Production and Infection of Cells") and maintained, respectively, in complete medium containing G418 (200 μg/ml) and G418 plus puromycin. The retroviral packaging cell line Phoenix 293 was grown in RPMI 1640 medium containing 5% defined fetal bovine serum as described previously (24). HeLa cells were grown in Dulbecco's modified Eagle's medium containing 5% fetal bovine serum.

Plasmids, Retroviral Vectors, and Other Recombinant DNA Constructs—Retroviral vectors, LXSN, LXSNCx32S, and LXSNCx43S, containing rat Cx32 and Cx43 cDNAs, respectively, were constructed as described previously (24–26). The carboxyl-terminally tagged pCx43-EYFP was constructed in the pEYFP-N1 vector as described previously (25). Carboxyl-terminally tagged pCx32-EYFP was constructed as described previously (27). Untagged carboxyl-terminally truncated pCxΔ233, pCxΔ257, and pCxΔ363 and carboxyl-terminally tagged truncated pCx43Δ233-EYFP and pCx43Δ257-EYFP were engineered in the pcDNA3.1 and pEYFP-N1 vector using standard PCR-based cloning methods using LXSNCx43S as a template. The PCR amplifications were performed using the forward 5′-GCCTCGAGATGGGTGACTGGAGT-3′ and the reverse primers 5′-CCGTGGATCCCTGAAGAAGACGTA-3′ (for pCx43Δ233-EYFP), 5′-CCGTGGATCCCTTGATGGGCTCAG-3′ (for pCx43Δ257-EYFP), and 5′-CCGTGGATCCACTGCTGGAAGGTCGTTGGTCCA-3′ (for pCx43Δ363). The forward and reverse primers, as underlined, were designed to contain XhoI and BamHI sites, respectively. The PCR products were first purified using QIAquick PCR purification kit (Qiagen, Valencia, CA) and, after digesting with XhoI and BamHI, were subcloned between XhoI- and BamHI-digested pEYFP-NI vector. pCx32Δ220-EYFP was constructed by PCR using LXSNCx32S as a template. For PCR, the following primers were used: forward primer 5′-GCCGAATTCATGAACTGGACAGGTC-3′ and the reverse primer 5′-CCGTGGATCCCAACGGCGGGCACAG-3′. The forward and reverse primers contained EcoRI and BamHI sites, respectively, as underlined. The purified PCR products were cloned into EcoRI/BamHI-digested pEYFP-NI. The entire coding sequences of EYFP-tagged full-length and truncated Cx43 and Cx32 chimeras were then subcloned into retroviral vector LXSN using standard recombinant DNA methodology. All recombinant DNA constructs were verified by DNA sequencing.

Transient Transfection—Phoenix 293T cells (1×10^6) were seeded in 10-cm dishes in 10 ml of complete medium. HeLa cells were seeded at a density of 2.5×10^5 cells per well in 2 ml of complete medium on glass coverslips in 6-well clusters or at a density of 7.5×10^5 cells per 6-cm dish in 4 ml of complete medium. Twenty four hour post-seeding, cells were transfected with appropriate plasmids using FuGENE 6 Transfection Reagent (Roche Diagnostics) as per the manufacturer's instructions with DNA (in micrograms) to FuGENE (in μl) ratio of 1:3. The medium was replaced with fresh medium 8 h post-transfection.

Retrovirus Production and Infection of Cells—Control and recombinant retroviruses harboring full-length and mutant Cxs and their EYFP-tagged chimeras were produced in Phoenix 293T cells as described previously (24). A431D and A431DE cells were multiply infected with various recombinant retroviruses and selected in either G418 (400 μg/ml) or in puromycin (2 μg/ml) for 2–3 weeks in complete medium. Glass cylinders were used to isolate individual antibiotic-resistant clones, which were expanded, frozen, and maintained in G418 (200 μg/ml) and in G418 and puromycin (2 μg/ml).

Cell Surface Biotinylation Assay—Cells (5×10^5) were seeded in 6-cm dishes in 4 ml of complete medium and grown to 80–90% confluence. Cell surface biotinylation was performed at 4 °C. In brief, cells were incubated with freshly prepared EZ-Link™Sulfo-NHS-SS biotin reagent (Pierce) at 0.5 mg/ml in phosphate-buffered saline (PBS) supplemented with 1 mM $CaCl_2$ and 1 mM $MgCl_2$ (PBS-PLUS) for 1 h. The reaction was quenched with PBS-PLUS supplemented with 20 mM glycine. Cell lysis and affinity precipitation of biotinylated proteins were performed as described previously (28) with the following modification. After cell lysis, 100 μg of total protein was incubated with 50 μl of streptavidin-agarose beads (Pierce) on a rotator overnight at 4 °C. The streptavidin-bound biotinylated proteins were eluted by incubating the beads for 30 min in 1×

Downloaded from www.jbc.org at Lehigh University, on November 10, 2010

SDS loading buffer. The samples were resolved by SDS-PAGE followed by Western blotting using appropriate antibodies. As an input, an equal amount of total protein (10 μg) was also subjected to SDS-PAGE and Western blot analysis. Protein concentration was determined using BCA reagent (Pierce).

Detergent Extraction and Western Blot Analysis of Connexin43 and Connexin32—Cell lysis, detergent solubility assay with Triton X-100, and Western blot analysis were performed as described previously (24, 28). In brief, 1×10^6 cells were seeded per 10-cm dish in 10 ml of complete medium and grown to confluence. Cells were then lysed in buffer SSK (10 mM Tris, 1 mM EGTA, 1 mM phenylmethylsulfonyl fluoride, 10 mM NaF, 10 mM *N*-ethylmaleimide, 10 mM Na_2VO_4, 10 mM iodoacetamide, 0.5% Triton X-100, pH 7.4) supplemented with the protease inhibitor mixture (Sigma). For the detergent solubility assay, the concentration of Triton X-100 was raised to 1% before ultracentrifugation at 100,000 × *g* for 60 min (35,000 rpm in analytical Beckman ultracentrifuge; model 17-65 using an SW50.1 rotor). The detergent-insoluble pellets were dissolved in buffer C (70 mM Tris/HCl, pH 6.8, 8 M urea, 10 mM *N*-ethylmaleimide, 10 mM iodoacetamide, 2.5% SDS, and 0.1 M dithiothreitol). Following normalization based on cell number, the total Triton X-100-soluble and -insoluble fractions were mixed with 4× SDS-loading buffer to a final concentration of 1× and boiled at 100 °C for 5 min (for Cx43) or incubated at room temperature for 1 h (for Cx32) before SDS-PAGE analysis.

Gene Knockdown by RNA Interference—SMARTpool siRNA against ZO-1 (TJP-1; catalogue no. L-007746-00) and DY-547-labeled siGLO RISC-free control siRNA (catalogue no. D-001600-01) were obtained from Thermo Fisher Scientific/Dharmacon RNA Interference Technologies. DY-547-labeled siGLO Lamin A/C siRNA (catalogue no. 001620-02) was used as a positive control. The 40 μM stock solution of the oligonucleotides was prepared using 1× siRNA buffer (Thermo Fisher Scientific). A431D-43 and A431DE-43 cells, seeded on glass coverslips in 12-well clusters, 8×10^4 cells/well, were transfected with the oligonucleotides using Oligofectamine (Invitrogen) as per the manufacturer's instructions. The final concentration of the oligonucleotides in each experiment was 130 nM. The efficiency of knockdown was assessed by immunoblotting and immunocytochemical analyses 72 h post-transfection. The final concentrations of the oligonucleotides as well as the duration of treatment were empirically determined from several pilot experiments.

Detergent (Triton X-100) Extraction of Cells in Situ—Live cells were extracted *in situ* with 1% Triton X-100 essentially as described previously (28). In brief, 2.5×10^5 cells were seeded per well in 6-well clusters containing glass coverslips. After 24 h, the cells were rinsed once in PBS and then incubated in isotonic medium (30 mM HEPES, pH 7.2, 140 mM NaCl, 1 mM $CaCl_2$, 1 mM $MgCl_2$, 300 mM sucrose) supplemented with the protease inhibitor mixture (Sigma) for 60 min at 4 °C in the presence and absence of 1% Triton X-100. The dishes were gently swirled intermittently. Following incubation, cells were fixed and immunostained with appropriate primary and secondary antibodies as described below.

Antibodies and Immunostaining—Rabbit polyclonal antibody against Cx43 and hybridoma M12.13 (a gift from Dr. Dan Goodenough, Harvard University) have been described earlier (26). Rabbit anti-EEA-1 (PA1-063) was obtained from Affinity BioReagents (Golden, CO). Mouse anti-occludin (clone OC-3F10) was from Zymed Laboratories Inc.. Rabbit anti-α-catenin, rabbit anti-β-catenin, rabbit anti-Cx32, and mouse anti-β-actin (clone C-15) antibodies were from Sigma. Mouse anti-ZO1 (610967) and mouse anti-GM130 (610822) antibodies were obtained from BD Transduction Laboratories. Rabbit anti-green fluorescent protein antibody (A6455) and Alexa Fluor 350-conjugated phalloidin were obtained from Invitrogen. Mouse anti-E-cadherin, mouse anti-α-catenin, and mouse anti-β-catenin antibodies have been described previously (19, 24, 29). We also used many other antibodies, both mouse monoclonal and rabbit polyclonal, against Cx43 to detect various phosphorylated forms. These antibodies are described in supplemental Fig. S3 legend.

Cells were immunostained after fixing with 2% paraformaldehyde for 15 min as described previously (24). In brief, 2.5×10^5 cells were seeded per well in 2 ml of complete medium in 6-well clusters containing glass coverslips. After 48 h, cells were fixed and immunostained at room temperature with various antibodies at appropriately calibrated dilutions. Secondary antibodies (rabbit or mouse) conjugated with Alexa Fluor 488 and Alexa Fluor 594 were used as appropriate. Images of immunostained cells were acquired with Leica DMRIE microscope (Leica Microsystems, Wetzler, Germany) equipped with Hamamatsu ORCA-ER CCD camera (Hamamatsu City, Japan) using 63× oil objective (NA 1.35). For co-localization studies, serial *z*-sections (0.3–0.5 μm) were collected and analyzed using image-processing software (Openlab 4.0 and Volocity 4.2.2, Improvision, Lexington, MA). SlowFade (Invitrogen) was used to mount cells on glass slides.

Cell Growth on Semi-permeable Filters—Approximately 4×10^4 cells were plated onto 12-mm Transwell filters (pore size, 0.4 μm; Corning Glass) in complete medium and grown for 3–6 days. Medium of the upper and lower filter chambers was changed on alternate days. The *in situ* detergent extraction and immunocytochemical analyses were performed directly on filters as described above for cells grown on glass coverslips. After immunostaining, the filters were cut with a sharp scalpel and mounted as follows. The filters were placed on glass slides with their cell side facing up and a drop of SlowFade was placed on top followed by a glass coverslip, which was pressed gently using a 50-g weight overnight. The edges were sealed with nail polish.

Cell Aggregation Assay—The hanging drop suspension culture method was used to test aggregation of parental and Cx-expressing A431D and A431DE cells as described previously (30). Cells were harvested with trypsin/EDTA and resuspended at 2.5×10^5 cells per ml in complete culture medium. A 20-μl drop of medium, containing 5×10^3 cells, was suspended as a hanging drop from the lid of a 10-cm^2 Petri dish (40 hanging drops per lid). The dish was filled with 10 ml of PBS to prevent drying of the drops. The cells were then allowed to aggregate in a humidified 5% CO_2 incubator at 37 °C for 14–16 h. At the end of the incubation, cells and aggregates were triturated 10 times

Downloaded from www.jbc.org at Lehigh University, on November 10, 2010

through a standard 200-μl pipette tip to disperse loosely associated cells, and a coverslip was placed gently on top of the cells. The cells were visualized by phase-contrast light microscopy using a 5× objective, and images were captured using a CCD camera (Retiga 2000R, FAST 1394), mounted on Leica DMIRE2 microscope, with the aid of Volocity (Improvision, Lexington, MA). For quantifying the size, the outline of each aggregate was drawn using an ROI tool of the AlphaDigiDoc 1201 software, and the area of each aggregate was measured. All images were analyzed at the same magnification, and the area was recorded as "relative units" for each aggregate. The average area of the aggregates was considered as a measure of aggregate formation and was determined from 30–35 aggregates.

Gap Junctional Communication Assays—Gap junctional communication was measured by microinjecting the fluorescent tracers Alexa Fluor 488 (570 Da; A-10436) and Alexa Fluor 594 (760 Da; A-10438). The Alexa dyes were obtained from Invitrogen, and their stock solutions (10 mM) were prepared in water as described previously (24). These fluorescent tracers were microinjected into test cells using Eppendorf InjectMan and FemtoJet microinjection systems (models 5271 and 5242, Brinkmann Instrument, Westbury, NY) mounted on a Leica DMIRE2 microscope as described previously (24). The microinjected cells were viewed and images captured using a CCD camera (Retiga 2000R, FAST 1394) with the aid of Volocity (Improvision, Lexington, MA). The captured images were stored as TIFF files and processed using Corel Photopaint (Ottawa, Ontario, Canada). Gap junctional communication was quantified as described previously (24–26).

Cytochalasin B Treatment—The stock solution of cytochalasin B (Sigma) was prepared in ethanol at 10 mg/ml and was stored at −20 °C in small aliquots. Cells, seeded on glass coverslips, were treated for 1–6 h at 37 °C with cytochalasin B at 1 μg/ml, which was appropriately diluted in cell culture medium to give the desired concentration. Controls were treated with ethanol alone.

Gap Junction Size Measurement—The length and area of a GJ plaque were measured after *in situ* extraction of cells with 1% Triton X-100, which removes Cxs and connexons that are not incorporated into GJs (28), and immunostaining with Cx43 antibody as described above (see under "Detergent Extraction and Western Blot Analysis of Connexin43 and Connexin32"). Images of immunostained cells were acquired with a Leica DMRIE microscope (Leica Microsystems, Wetzler, Germany) equipped with Hamamatsu ORCA-ER CCD camera (Hamamatsu City, Japan) using a 63× oil objective (NA 1.35). Serial *z*-sections (0.5 μm) were collected and subjected to iterative volume deconvolution using Volocity image-processing software (Improvision, Lexington, MA). Single optical section of the deconvolved image was used for measuring GJ size. Each distinct punctum seen at the cell-cell contact site was considered as one GJ plaque. The area of each GJ plaque was analyzed by drawing an ROI around each distinct punctum using the "magic wand" tool of the "Measurement" module of Volocity. The area of each GJ is represented as "pixel count," and one pixel corresponds to 0.01 μm^2. In each captured image, 3–5 puncta were randomly chosen for the measurement of area and length, and between 5 and 15 images were used. For the measurement of GJ length, we used the "line" tool of the measurement module of Volocity to ascribe the farthest visible points along the long axis of each GJ punctum. The length is represented in relative units where "a unit" corresponds to 0.1 μm. For determining the number of GJ plaques per cell-cell interface, we used the "merge planes" command of Volocity to merge all planes obtained during *Z*-sections. We then counted the number of distinct visible puncta along the cell-cell interfaces of two adjoining cells. Only distinct interfaces were chosen for these measurements at random to avoid ambiguity with regard to the localization of the puncta, and 60–70 interfaces were measured from three independent experiments.

Statistical Analysis—The statistical significance between groups was calculated by standard Student's *t* test using means ± S.E. and the entire sample size. These values were calculated using SigmaPlot 11 (Systat Software, Inc., San Jose, CA).

RESULTS

Differential Assembly of Connexin43 and Connexin32 into Gap Junctions—A431D cells, derived from human squamous carcinoma cell line A431, are devoid of E-cadherin or N-cadherin. Moreover, although the expression of desmosomal cadherins (desmocollins and desmogleins) was not affected, A431D cells do not form adherens junctions, desmosomes, and tight junctions and are devoid of cell-cell adhesion. Furthermore, the half-life of adherens junction-associated proteins, α- and β-catenin, is severely reduced (19, 20). We introduced Cx43 and Cx32 into cadherin-null (A431D) and E-cadherin-expressing (A431DE) cells using recombinant retroviruses LXSNCx43S and LXSNCx32S as described previously (24, 26). A431D cells do not express these Cxs detectably. Fig. 1 shows the expression level of Cx43 (*C*) and Cx32 (*D*) in representative clones derived from cadherin-null A431D (A431D-43 and A431D-32) and cadherin-expressing A431DE (A431DE-43 and A431DE-32) cells. These clones were chosen on the basis of equal expression of both Cxs and E-cadherin as assessed by the densitometric scanning of Western blots. For the sake of simplicity, these clones will be referred to as cells in subsequent studies. Immunocytochemical analysis showed that Cx43 assembled into GJs both in cadherin-null A431D-43 and E-cadherin-expressing A431DE-43 cells (Fig. 1*A*, *upper panels*), whereas Cx32 failed to assemble into GJs and appeared to form intracellular aggregates of variable size both in A431D-32 and A431DE-32 cells (Fig. 1*A*, *lower panels*).

In E-cadherin-expressing A431DE-43 cells, Cx43 clearly appeared to form larger GJs as compared with cadherin-null A431D-43 cells (Fig. 1*A*, compare the size of GJ puncta in *upper left panel* with the *right panel*). We therefore determined the size and area of 100–200 individual gap junctional puncta (supplemental Fig. S1) as well as the mean number of gap junctional puncta per cell-cell interface in A431D-43 and A431DE-43 cells (supplemental Fig. S2). The size of each fluorescent spot or punctum at the interface was presumed to represent a single GJ plaque (31). These measurements showed that the mean area and the length of GJ plaques increased nearly 2-fold (supplemental Fig. S1), and the mean number of GJ puncta per interface was decreased 2-fold (supplemental Fig. S2) in

Downloaded from www.jbc.org at Lehigh University, on November 10, 2010

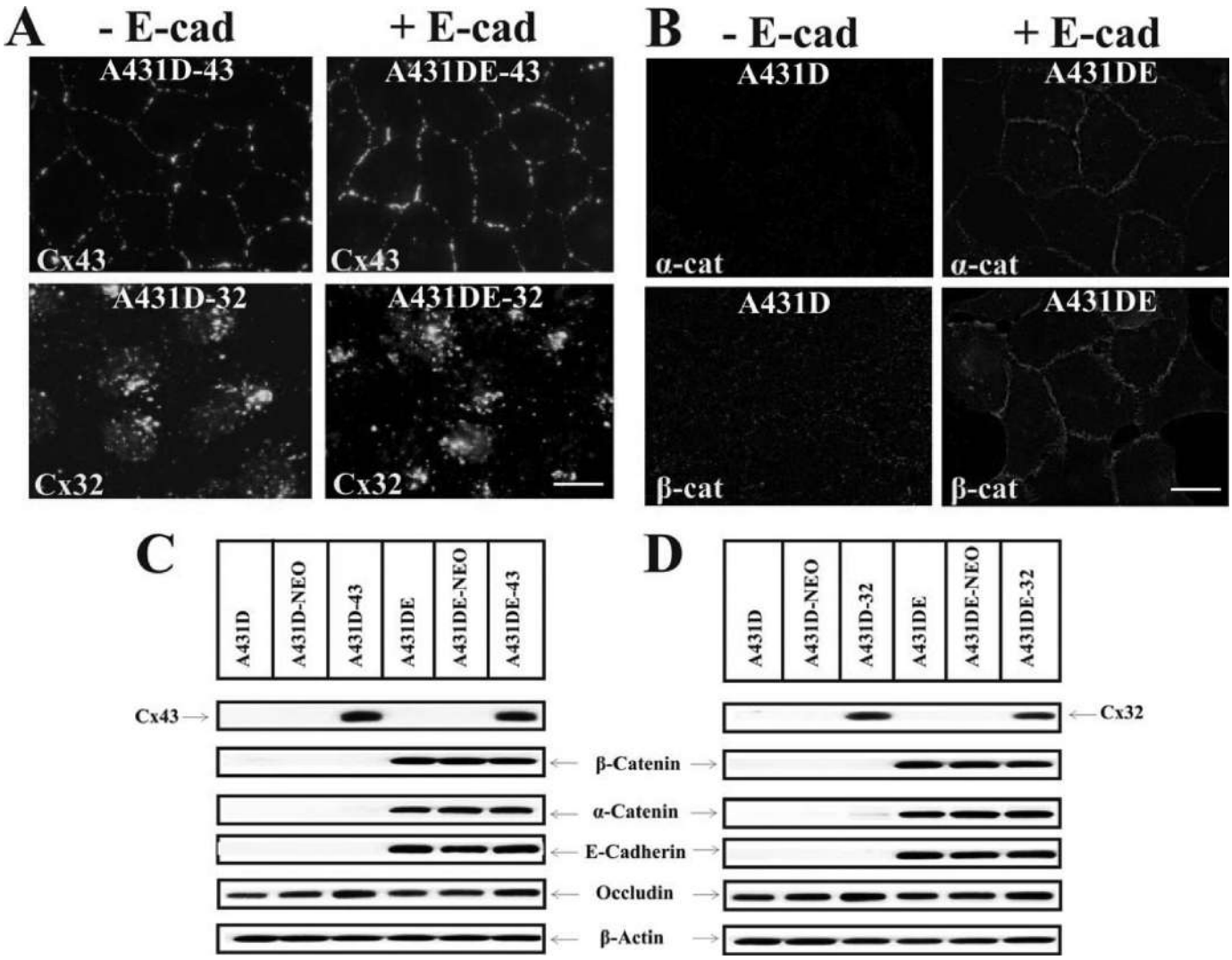

FIGURE 1. **Isolation of A431D and A431DE clones expressing equal levels of connexin32 and connexin43.** A431D and A431DE cells were infected with LXSN, LXSNCx32S, and LXSNCx43S and selected as described (see under "Materials and Methods"). *A,* localization of Cx43 and Cx32 by immunocytochemical analyses. A431D-43, A431DE-43, A431D-32, and A431DE-32 cells were immunostained for Cx43 and Cx32. Note that Cx43 assembles into GJs in the absence (−*E-cad*) and in the presence (+*E-cad*) of E-cadherin (*E-cad*), whereas Cx32 remains intracellular and fails to assemble. Note also that Cx43 forms larger GJs in E-cadherin-expressing cells. *B,* E-cadherin expression recruits α-catenin (*α-cat*) and β-catenin (*β-cat*) to cell-cell contact areas. A431D and A431DE cells were immunostained for α- and β-catenins. Note localization of both catenins at cell-cell contact areas in A431DE but not in A431D cells. *C* and *D,* expression level of Cx43 (*C*) and Cx32 (*D*) and E-cadherin, β-catenin, α-catenin, and occludin in parental (A431D and A431DE) cells and in cells infected with LXSN (A431D-NEO and A431DE-NEO), LXSNCx43S (A431D-43 and A432DE-43), and LXSNCx32S (A431D-32 and A431DE-32). Ten micrograms of total protein was resolved on 12% SDS-PAGE and immunoblotted for Cx32, Cx43, E-cadherin, β-catenin, α-catenin, and occludin. The blots were re-probed with β-actin to verify equal loading. Note that Cx43 (*C*) and Cx32 (*D*) are expressed only in clones infected with LXSNCx32S and LXSNCx43S, respectively. Note that expression of E-cadherin, α-catenin, and β-catenin is detected only in A431DE clones. *Bar,* 15 μm.

A431DE-43 cells compared with A431D-43 cells. It is worth noticing that the polyclonal antibody used to probe these blots (catalogue no. 6219, Sigma) predominantly detected only one major form of Cx43 in A431D-43 and A431DE-43 cells and in other cell lines that differ widely in their capacity to form GJs used in our earlier studies (supplemental Fig. S3). However, both phosphorylated and nonphosphorylated bands were detected when the blots were probed with anti-Cx43 antibody raised against residues 252–271 (both monoclonal and polyclonal) or with other antibodies, some of which were phospho-specific (supplemental Fig. S3). Although the resolving power of the SDS-polyacrylamide gels did not permit us to establish a correlation between a specific phosphorylated form of Cx43 and its ability to assemble into GJs, the above data suggest that, as is observed in several other cell lines that assemble GJs, Cx43 in A431D-43 and A431DE-43 cells is phosphorylated similarly before its assembly into GJs.

Consistent with the earlier studies (19), E-cadherin expression also stabilized adherens junction-associated proteins α- and β-catenins (Fig. 1, *C* and *D*), and recruited them to cell-cell contact areas (Fig. 1*B*, compare *left panels* with the *right panels*). Expression of Cx43 and Cx32 neither induced nor modulated E-cadherin-mediated cell-cell adhesion in cadherin-null and E-cadherin-expressing cells as assessed by conventional hanging drop assay (supplemental Fig. S4). This assay measures the rate and strength of cell-cell adhesion based on the sizes of cell aggregates formed over time from single cells as well as the resistance of the formed aggregates to a shearing force

Downloaded from www.jbc.org at Lehigh University, on November 10, 2010

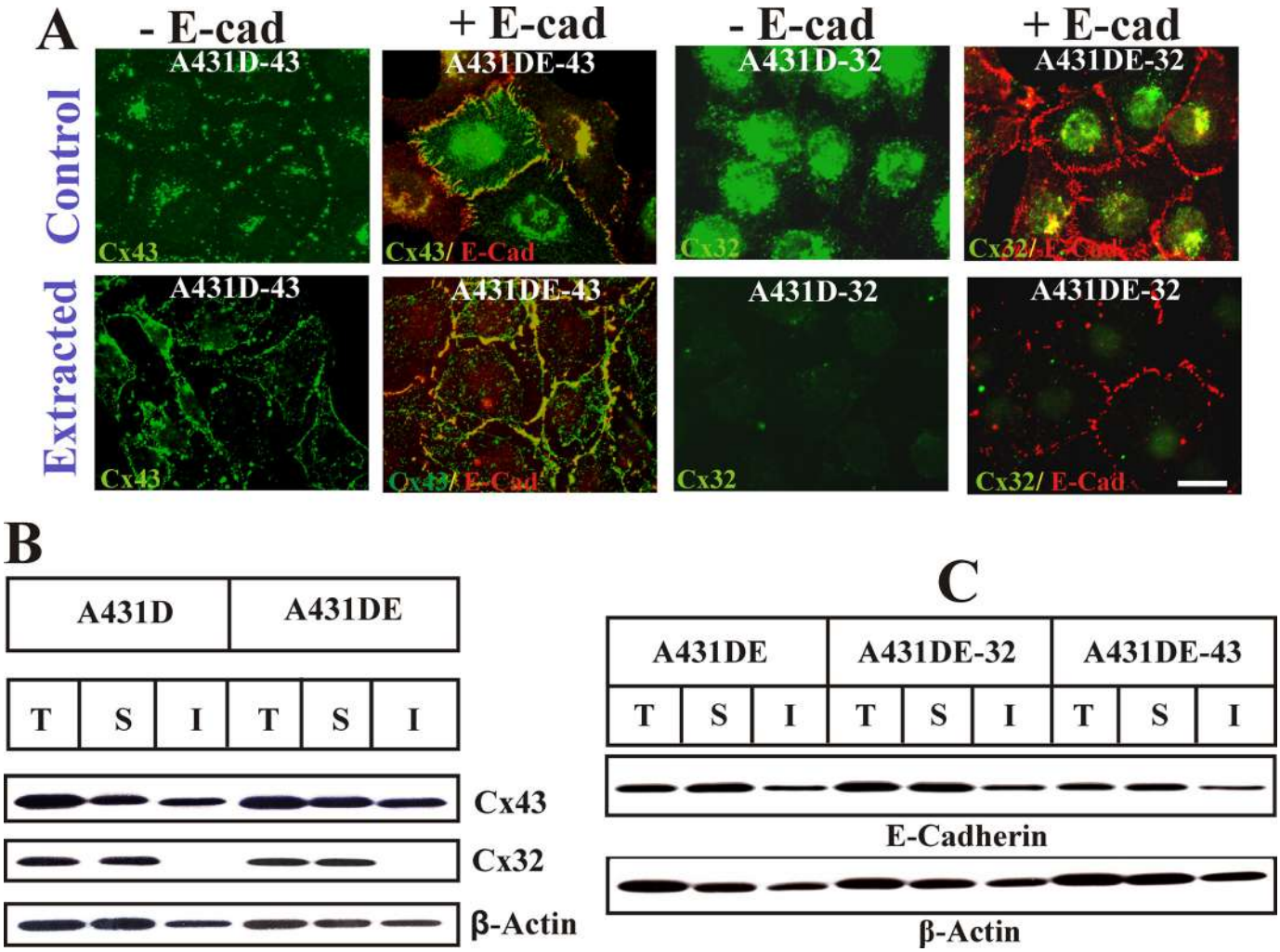

FIGURE 2. **Detergent-solubility of connexin32 and connexin43 in A431D and A431DE cells.** *A,* assembly of Cxs into GJs was examined in A431D-43, A431DE-43, A431D-32, and A431DE-32 cells upon *in situ* extraction with 1% Triton X-100 at 4 °C (see under "Materials and Methods"). Cells were immunostained for Cx32/Cx43 (*green*) and E-cadherin (*red*). Note the disappearance of intracellular, but not junctional, Cx43 and E-cadherin (*E-cad*) upon extraction. Note also the larger size of Cx43 puncta in A431DE-43 cells and their significant co-localization with E-cadherin under control and Triton X-100-extracted conditions. *B,* total (*T*), Triton X-100-soluble (*S*), and Triton X-100-insoluble (*I*) fractions from A431D-43, A431DE-43, A431D-32, and A431DE-32 were analyzed by Western blot analysis (see under "Materials and Methods"). Note that although Cx43 is detected in the both detergent-soluble and -insoluble fractions, Cx32 is detected only in the soluble fraction, and E-cadherin expression has no detectable effect on detergent solubility of Cx43. The blots were stripped and re-probed with anti-β-actin antibody as a loading control. *C,* connexin expression does not affect the detergent solubility of E-cadherin. Total, Triton X-100-soluble and -insoluble fractions from A431DE, A431DE-43, and A431DE-32 cells were analyzed by Western blot analysis (see under "Materials and Methods"). Note that similar levels of E-cadherin are detected in the detergent-insoluble fraction in all cells. The blots were stripped and re-probed with anti-β-actin to verify equal loading. *Bar,* 10 μm.

TABLE 1

Junctional communication of various fluorescent tracers in connexin43-expressing cells with or without E-cadherin

Tracer	Exp. no.	A431D-43	A431DE-43	*p* value
Lucifer Yellow (443 Da)	1	33 ± 4[a] (22)[b]	32 ± 5 (24)	0.878
	2	29 ± 4 (30)	35 ± 4 (30)	0.301
Alexa Fluor 488 (570 Da)	1	18 ± 3 (28)	21 ± 4 (32)	0.560
	2	16 ± 3 (26)	19 ± 3 (40)	0.502
Alexa Fluor 594 (60 Da)	1	4 ± 1 (28)	5 ± 1 (29)	0.483
	2	6 ± 2 (34)	7 ± 2 (30)	0.726

[a] Mean number of fluorescent cells 5 min after microinjection ± S.E. is shown.
[b] Number of microinjection trials is shown.

(30, 32). Only E-cadherin-expressing cells aggregated efficiently (supplemental Fig. S4, *A, lower panels*; see also *B*), whereas cadherin-null cells with or without Cx expression did not (supplemental Fig. S4, *A, upper panels*; see also *B*).

E-Cadherin Expression and the Detergent Solubility of Connexin43 and Connexin32—To corroborate the immunocytochemical data, we measured the assembly of Cx43 and Cx32 into GJs biochemically (Fig. 2*B*), by detergent insolubility assay (28), and functionally, by measuring the junctional transfer of fluorescent tracer Alexa Fluor 488 (570 Da), Lucifer Yellow (443 Da) and Alexa Fluor 594 (760 Da) (supplemental Fig. S5 and Table 1). Moreover, we also examined the detergent solubility of both Cxs upon *in situ* extraction of live cells with 1% Triton X-100 (Fig. 2*A*). As expected, a significant proportion of Cx43 remained insoluble in 1% Triton X-100 in A431D-43 and A431DE-43 cells (Fig. 2*A*, compare control and extracted in *1st* and *2nd columns*, and *B, top blot*, *T* = total, *S* = soluble, and *I* = insoluble fractions), whereas no insoluble fraction of Cx32 was detected in cadherin-null A431D-32 or E-cadherin-expressing A431DE-32 cells (Fig. 2*A*, compare control and extracted in

Downloaded from www.jbc.org at Lehigh University, on November 10, 2010

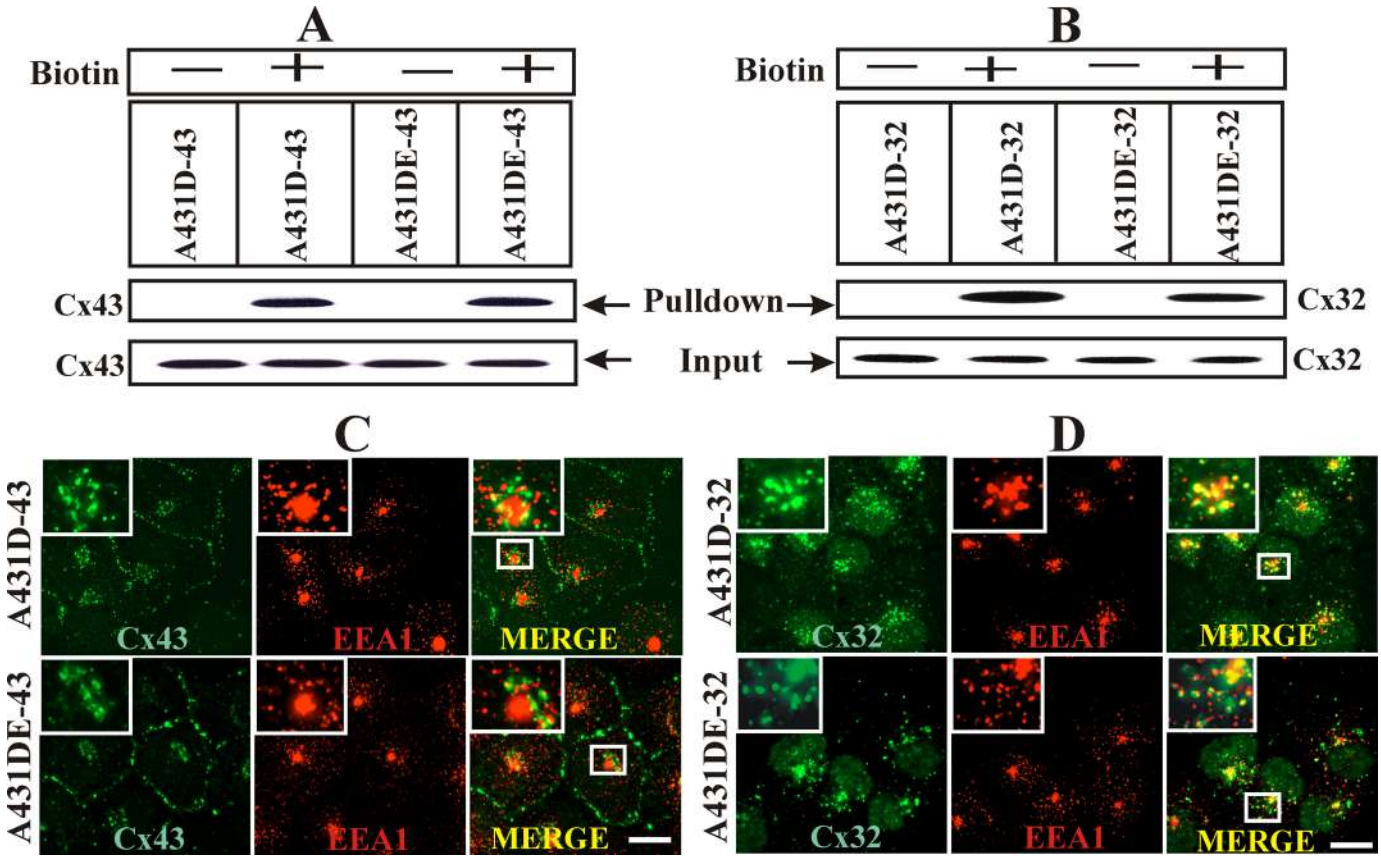

FIGURE 3. **E-cadherin expression does not affect trafficking and subcellular localization of connexin43 and connexin32.** *A* and *B*, cell-surface biotinylation of Cx43 and Cx32 in A431D and A431DE cells. Confluent A431D-43 and A431DE-43 (*A*) and A431D-32 and A431DE-32 cells (*B*) were biotinylated with sulfo-NHS-SS-biotin at 4 °C, and biotinylated Cxs from 100 μg of total protein were detected by streptavidin pulldown followed by Western blotting (see under "Materials and Methods"). As an input, 10 μg of total protein was used and probed for Cx43 or Cx32. Note that in both A431D-43 and A431DE-43 cells (*A*; labeled as + Biotin) and A431D-32 and A431DE-32 cells (*B*; labeled as + *Biotin*), similar levels of Cx43 and Cx32 were detected in the streptavidin *Pulldown lanes*, respectively. A nonbiotinylated dish (labeled as − *Biotin*) was used as a negative control. *C* and *D*, co-localization of Cx43 and Cx32 with EEA-1 in A431D-43 and A431DE-32 and A431DE-43 and A431DE-32 cells. Note the co-localization of both Cx43 (*C*) and Cx32 (*D*, *green*) with EEA1 (*red*) in all cells. Note extensive co-localization of Cx32 with EEA1. The *boxed region* is magnified and shown in the *inset*. *Bar*, 15 μm.

2nd and *4th columns*, and *B*, *middle blot*). Under similar conditions, the detergent solubility of E-cadherin was not significantly affected as assessed by *in situ* extraction (Fig. 2*A*, compare control and extracted, *2* and *4 columns*) and by Western blot analysis (Fig. 2*C*). In agreement with the immunocytochemical data, no junctional communication of Alexa Fluor 488 was detected in cadherin-null A431D and A431D-32 and E-cadherin-expressing A431DE and A431DE-32 cells (supplemental Fig. S5). On the other hand, Cx43-expressing cells communicated extensively, and cadherin expression had little effect on junctional communication (supplemental Fig. S5, *bottom panels*, and Table 1). Altogether, the data shown in Figs. 1 and 2 and supplemental Figs. S1–S4 suggest the following. 1) Cx43 is able to assemble into GJs in the absence of E-cadherin, but Cx32 is not. 2) E-cadherin-mediated cell-cell adhesion facilitates the assembly and growth of GJs composed of Cx43. 3) E-cadherin expression alone is not sufficient to induce the assembly of Cx32 into GJs *de novo*.

Trafficking and Subcellular Localization of Connexin43 and Connexin32 in the Presence and the Absence of E-cadherin—We next examined whether failure of Cx32 to form GJs was due to its impaired trafficking to the cell surface or a result of endocytosis prior to its assembly into GJs. We used cell-surface biotinylation to determine the trafficking of Cx43 and Cx32 to the cell surface and markers specific for the secretory and the endocytic pathways to examine their subcellular localization in cadherin-null and E-cadherin-expressing cells. As shown in Fig. 3, both Cx43 (Fig. 3*A*) and Cx32 (Fig. 3*B*) were biotinylated significantly in cadherin-null and cadherin-expressing cells. Connexin43 co-localized only partially with the early endocytic marker, EEA1 (Fig. 3*C*) (33), whereas Cx32 co-localized extensively (Fig. 3*D*). Both Cx43 and Cx32 co-localized with GM130 (supplemental Fig. S6), a marker for cis-Golgi (34) and Lamp-1 (data not shown), in cadherin-null and E-cadherin-expressing cells. Taken together, these data suggest that a significant fraction of Cx32 traffics to the cell surface both in the presence and absence of E-cadherin but in contrast to Cx43 is likely endocytosed prior to its assembly into GJs.

Assembly of Connexin32 into Gap Junctions Is Induced in A431D and A431DE Cells When Grown on Trans-Well-permeable Membrane Supports—In contrast to ubiquitous expression of Cx43, the expression of Cx32 is preferentially observed in well differentiated and polarized cells, such as hepatocytes and the secretory cells of exocrine glands (23). Permeable membrane supports have been widely used as surrogate substrates to mimic the milieu encountered by epithelial cells *in*

Downloaded from www.jbc.org at Lehigh University, on November 10, 2010

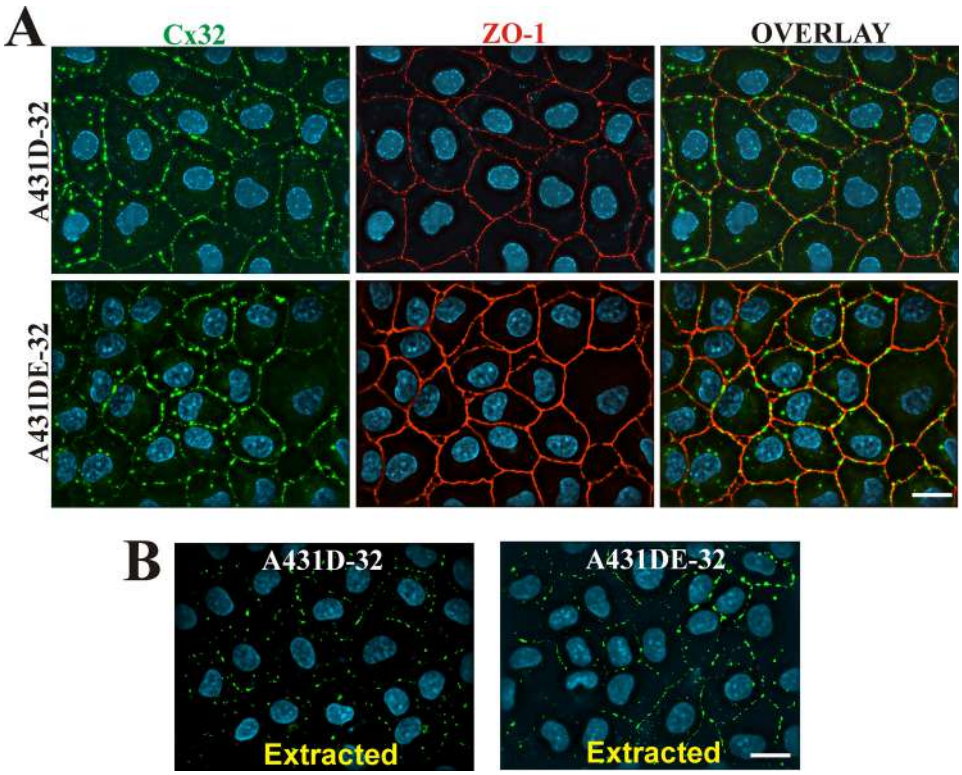

FIGURE 4. **Connexin32 assembles into gap junctions in A431D-32 and A431DE-32 cells grown on Transwell filters.** *A,* A431D-32 and A431DE-32 cells, seeded on clear Transwell filters, were grown for 5 days and immunostained for Cx32 (*green*) and ZO-1 (*red*) as described under "Materials and Methods." Note the formation of distinct GJ puncta at the cell-cell contact sites as delineated by ZO-1. Note lack of significant difference in the size and number of Cx32 puncta at the cell-cell contact sites between A431D-32 and A431DE-32 cells. Note also that the GJ puncta remain detergent-resistant (*B*). *Bar,* 15 μm.

TABLE 2

Junctional communication of various fluorescent tracers in cells grown on Transwell filters expressing connexin43 and connexin32 with or without E-cadherin

A431D-43, A431DE-43, A431D-32, and A431DE-32 cells were grown on 35-mm Transwell filters in replicate at a density of 2×10^5 cells per dish and allowed to grow to confluence for 5 days. Junctional communication was measured by microinjecting different fluorescent tracers as described under "Materials and Methods."

Cell line	Lucifer Yellow	Alexa Fluor 488	Alexa Fluor 594
A431D-32	0 ± 0^a (52)^b	0 ± 0 (39)	0 ± 0 (32)
A431DE-32	0 ± 0 (53)	0 ± 0 (47)	0 ± 0 (49)
A431D-43	31 ± 5 (22)^c	16 ± 4 (27)^d	6 ± 2 (26)^e
A431DE-43	34 ± 7 (25)^c	17 ± 5 (23)^d	7 ± 2 (32)^e

[a] Mean number of fluorescent cells 5 min after microinjection ± S.E. is shown.
[b] Number of microinjection trials is shown. There was no statistically significant difference in junctional communication between A431D-43 and A431DE-43 cells.
[c] Data are not significant; $p = 0.735$ for Lucifer Yellow.
[d] Data are not significant; $p = 0.875$ for Alexa Fluor 488.
[e] Data are not significant; $p = 0.728$ for Alexa Fluor 594.

vivo and to induce polarized and differentiated cell states (35). Hence, we investigated if the assembly of Cx32 into GJs could be induced upon growing cadherin-null A431D-32 and E-cadherin-expressing A431DE-32 cells on Transwell filters. When grown on Transwell filters for 3–6 days (see under "Materials and Methods"), A431D and A431DE cells became more columnar, as assessed by a 2-fold increase in cell height compared with cells grown on plastic or glass coverslips (supplemental Fig. S7, *A* and *B*), but failed to attain a fully polarized state as assessed by the random orientation of Golgi stacks (GM130 staining), distribution of β1-integrin, and Na-K-ATPase (supplemental Fig. S7*B*), and ZO-1 (supplemental Fig. S7*A, red*) at the apical and basolateral domains (35). However, despite incomplete polarization, Cx32 assembled into discrete GJ puncta (Fig. 4*A*), which remained Triton X-100-insoluble upon *in situ* extraction (Fig. 4*B*). Such puncta were not observed in cells grown on glass coverslips in parallel (supplemental Fig. S8*A*). As assessed visually, E-cadherin expression seemed to have little effect on the number and size of Cx32 GJs assembled in filter-grown A431D and A431DE cells (Fig. 4*A*).

We also found that the assembly of Cx43 into GJs appeared to be slightly enhanced when cadherin-null A431D-43 cells were grown on Transwell filters (supplemental Fig. S8*B*) as compared with cells grown on glass coverslips in parallel experiments (supplemental Fig. S8*C*); however, E-cadherin expression had no further effect (supplemental Fig. S8*B*). Also, neither the expression of E-cadherin in A431D cells nor punctate immunostaining characteristics of GJs were observed in parental A431D and A431DE cells grown on Transwell filters (data not shown). To assess if the detergent-resistant puncta represented functional GJs, we measured the junctional transfer of fluorescent tracers, Lucifer Yellow (443 Da), Alexa Fluor 488 (570 Da), and Alexa Fluor 594 (760 Da) by microinjection. Intriguingly, we found that filter-grown A431D-32 and A431DE-32 cells did not communicate (Table 2). These findings suggest that the filter-grown A431D-32 and A431DE-32 cells acquire a partially polarized physiological state that is conducive for the assembly of Cx32 into GJs, but the junctional channels stay closed and do not permit the passage of molecules ≥443 Da. Moreover, the data also suggest that assembly of Cx43 is enhanced upon partial polarization independent of E-cadherin expression when cells acquire a columnar phenotype.

Carboxyl Termini of Connexin43 and Connexin32 Are Required to Initiate Gap Junction Assembly in A431D Cells—The findings reported above showed that Cx43 was assembled into GJs in cadherin-null cells in the absence of measurable cell-cell adhesion, and E-cadherin-mediated cell-cell adhesion enhanced the assembly further. On the other hand, the assembly of Cx32 into GJs was contingent upon acquisition of partially polarized state. Because the carboxyl termini of Cx43 and Cx32 have been shown to interact with many proteins (21, 22, 36), we examined if they were required for GJ assembly in A431D and A431DE cells. To test this notion, we generated the following EYFP-tagged chimeras of Cx43 and Cx32: 1) Cx43-EYFP, which does

Downloaded from www.jbc.org at Lehigh University, on November 10, 2010

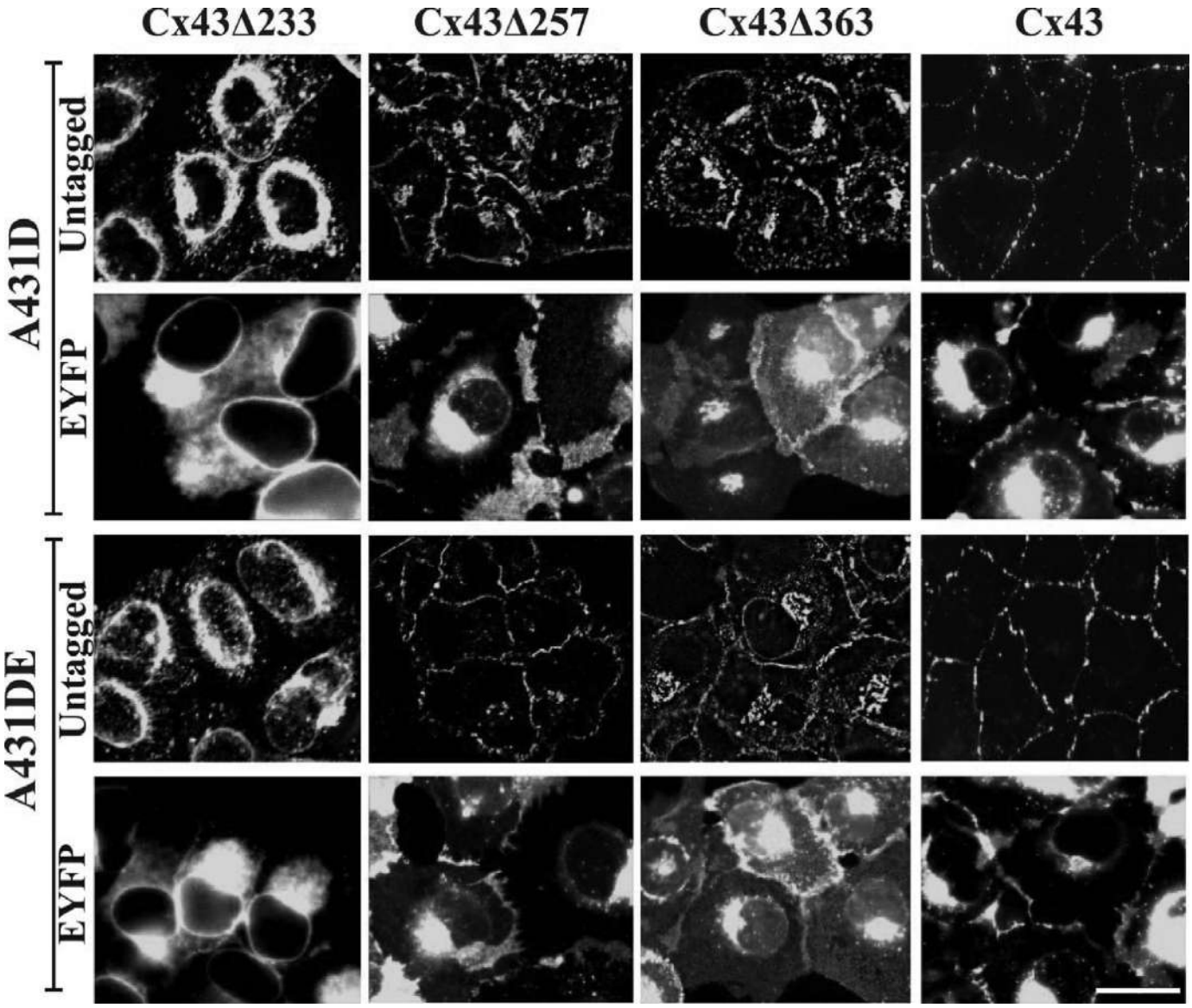

FIGURE 5. **Carboxyl-terminally truncated untagged and EYFP-tagged chimeras of Cx43 fail to assemble into gap junctions.** Polyclonal cultures of A431D and A431DE cells expressing Cx43Δ233, Cx43Δ233-EYFP, Cx43Δ257, Cx43Δ257-EYFP, Cx43Δ363, Cx43Δ363EYFP, Cx43, and Cx43-EYFP were grown on glass coverslips. Cells expressing untagged Cx43 and truncated mutants were immunostained with polyclonal antibody raised against amino acid residues 252–271 of Cx43 (see under "Materials and Methods"). Note that all truncated and EYFP-tagged chimeras of Cx43 remain intracellular, whereas untagged Cx43 is assembled into GJs in cadherin-null (A431D) and E-cadherin-expressing (A431DE) cells. Note that the localization pattern of untagged *versus* EYFP-tagged full-length and mutant Cx chimeras appears to be different partly due to the brighter diffuse EYFP fluorescence of tagged Cx mutants compared with untagged Cx mutants, which were detected immunocytochemically. All EYFP-tagged and carboxyl-terminally truncated mutants are lost upon *in situ* extraction (data not shown). *Bar,* 10 μm.

not bind to the second PDZ domain of ZO-1 (37); 2) Cx43Δ363, from which ZO-1 binding domain has been deleted (38, 39); 3) Cx43Δ257, from which 135 amino acids that harbor most of the potential phosphorylation sites and the known interacting motifs, including the ZO-1-binding site, have been deleted; 4) Cx43Δ257-EYFP; 5) Cx43Δ233, from which 159 amino acids comprising the entire carboxyl terminus have been deleted, including the tubulin-binding site (38, 39); 6) Cx43Δ233-EYFP; 7) Cx32-EYFP; 8) Cx32Δ220, which assembles into GJs but is devoid of most of the carboxyl terminus (24); and 9) Cx32Δ220-EYFP.

Cadherin-null A431D and E-cadherin-expressing A431DE cells were infected with the recombinant retroviruses harboring these chimeras, along with the untagged Cx43 and Cx32, and the formation of GJs was investigated immunocytochemically in polyclonal cultures, pooled from 50 to 100 clones, within four to six population doublings. In addition, the same chimeras were also introduced into HeLa cells, which have been widely used to examine the assembly of various Cxs into GJs (7, 40, 41), and into LNCaP prostate cancer cells used in our laboratory (24). We found that chimeras Cx43-EYFP, Cx43Δ363, Cx43Δ257, Cx43Δ257-EYFP, Cx43Δ233, and Cx43Δ233-EYFP failed to assemble into GJs in A431D and A431DE cells seeded on glass coverslips and remained either intracellularly or diffusely distributed at the regions of cell-cell contact (Fig. 5) as compared with untagged Cx43 (Fig. 5, *4th column*; see also Figs. 1–3). Moreover, all truncated, untagged, and EYFP-tagged mutants and chimeras of Cx43 could be extracted with 1% Tri-

Downloaded from www.jbc.org at Lehigh University, on November 10, 2010

ton X-100, suggesting that they had not assembled into GJs (data not shown). Functional studies showed that these cells did not permit the transfer of fluorescent tracer Alexa Fluor 488, Lucifer Yellow, and Alexa Fluor 594 (Table 3). We also found that, when grown on Transwell filters, Cx32Δ220 and Cx32Δ220-EYFP formed intracellular aggregates of variable size that appeared to be distributed throughout the cytoplasm both in A431D and A431DE cells (Fig. 6, *top panels*). Moreover, these aggregates or puncta were lost upon *in situ* extraction with 1% Triton X-100 (Fig. 6, *bottom panels*) as compared with full-length Cx32 (Fig. 4) and Cx32-EYFP which formed GJs (data not shown).

TABLE 3

Junctional communication of various fluorescent tracers in cells expressing wild-type and EYFP-tagged connexin43 chimeras with or without E-cadherin

A431D-43, A431DE-43, A431D-32, and A431DE-32 cells were grown on 35-mm Transwell filters in replicate at a density of 2×10^5 cells per dish and allowed to grow to confluence for 5 days. Junctional communication was measured by microinjecting different fluorescent tracers as described under "Materials and Methods."

Cell line	Lucifer Yellow	Alexa Fluor 488	Alexa Fluor 594
A431D-43	24 ± 5[a] (22)[b]	16 ± 3 (19)	7 ± 2 (20)
A431DE-43	26 ± 4 (21)[c]	17 ± 3 (29)[d]	8 ± 3 (18)[e]
A431D-43-EYFP	0 ± 0 (36)	0 ± 0 (37)	0 ± 0 (18)
A431D-43Δ257	0 ± 0 (23)	0 ± 0 (27)	0 ± 0 (23)
A431D-43Δ363	0 ± 0 (33)	0 ± 0 (42)	0 ± 0 (44)
A431DE-43-EYFP	0 ± 0 (20)	0 ± 0 (17)	0 ± 0 (22)
A431DE-43Δ257	0 ± 0 (24)	0 ± 0 (20)	0 ± 0 (18)
A431DE-43Δ363	0 ± 0 (23)	0 ± 0 (22)	0 ± 0 (24)

[a] Mean number of fluorescent cells 5 min after microinjection ± S.E. of the mean is shown.
[b] Number of microinjection trials is shown. There was no statistically significant difference in junctional communication between A431D-43 and A431DE-43 cells.
[c] Data are not significant; $p = 0.758$ for Lucifer Yellow.
[d] Data are not significant; $p = 0.823$ for Alexa Fluor 488.
[e] Data are not significant; $p = 0.779$ for Alexa Fluor 594.

Next, we investigated whether the assembly of these Cx43 chimeras could be induced upon growing cells on Transwell filters. We found that these chimeras failed to form GJs, remained intracellular or diffusely localized at the areas of cell-cell contact, and were lost upon *in situ* extraction with 1% Triton X-100 (supplemental Fig. S9, compare control and extracted). In contrast, Cx43-EYFP and Cx43Δ257-EYFP formed large GJs in HeLa and LNCaP cells (supplemental Fig. S10*A*), and Western blotting performed in HeLa cells confirmed that chimeric Cxs were stable and migrated at the predicted size (supplemental Fig. S10*B*). Consistent with the earlier studies (39), we found that Cx43Δ233-EYFP, in which the tubulin-binding site had been deleted, remained intracellular in HeLa cells (supplemental Fig. S10*A, left panels*). Moreover, in LNCaP cells, Cx32, Cx32-EYFP, Cx32Δ220, and Cx32Δ220-EYFP were expressed appropriately and formed GJs (supplemental Fig. S10*D*) (24). These data suggest that carboxyl terminus of Cx43 and Cx32 is required to form GJs in A431D cells.

Connexin43, ZO-1, and Actin Co-localize as Discrete Puncta at Cell-Cell Contact Sites—Previous studies showed that Cx43 interacted with the second PDZ domain of ZO-1 (39, 42). Addition of EYFP tag to full-length Cx43 has been shown to abolish its interaction with ZO-1 (37). Moreover, the interaction of ZO-1 with Cx43 has been shown to influence GJ assembly and dynamics (22). Because chimeras Cx43-EYFP and Cx43Δ257-EYFP failed to form GJs in A431D-43 and A431DE-43 cells, but formed larger GJs in HeLa and LNCaP cells, we studied the subcellular localization of ZO-1 and Cx43 in cells expressing full-length Cx43 and EYFP-tagged chimeras in A431D-43 and

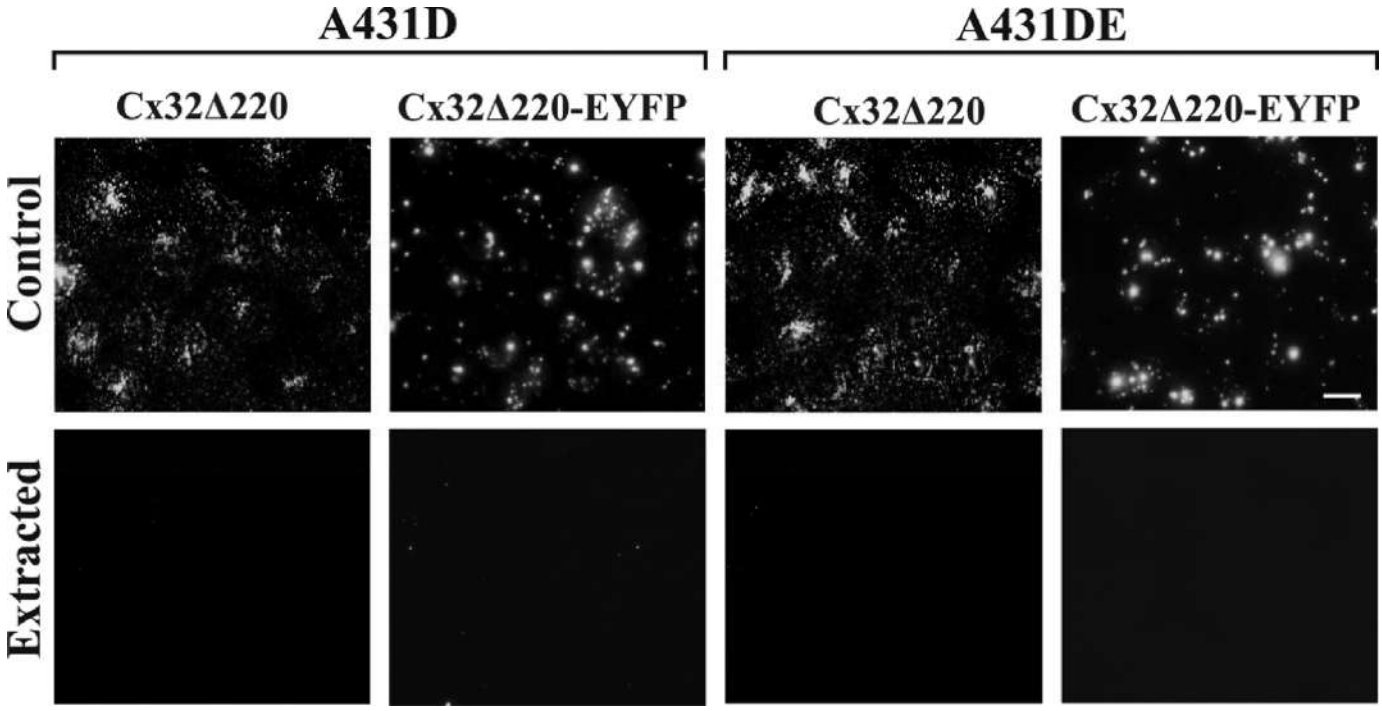

FIGURE 6. **Carboxyl-terminally truncated untagged and EYFP-tagged chimera of Cx32 fail to assemble into gap junctions.** Polyclonal cultures of A431D and A431DE cells expressing Cx32Δ220 and Cx32Δ220-EYFP were grown on Transwell filters and were extracted *in situ* with 1% Triton X-100 (see under "Materials and Methods"). Note that both Cx32Δ220 and Cx32Δ220-EYFP remain as scattered intracellular puncta or aggregates that are lost upon detergent extraction. Note that the localization pattern of untagged *versus* EYFP-tagged full-length and mutant Cx chimeras appears to be different partly due to the brighter diffuse EYFP fluorescence of tagged Cx mutants compared with untagged Cx mutants, which were detected immunocytochemically. *Bar,* 20 μm.

Downloaded from www.jbc.org at Lehigh University, on November 10, 2010

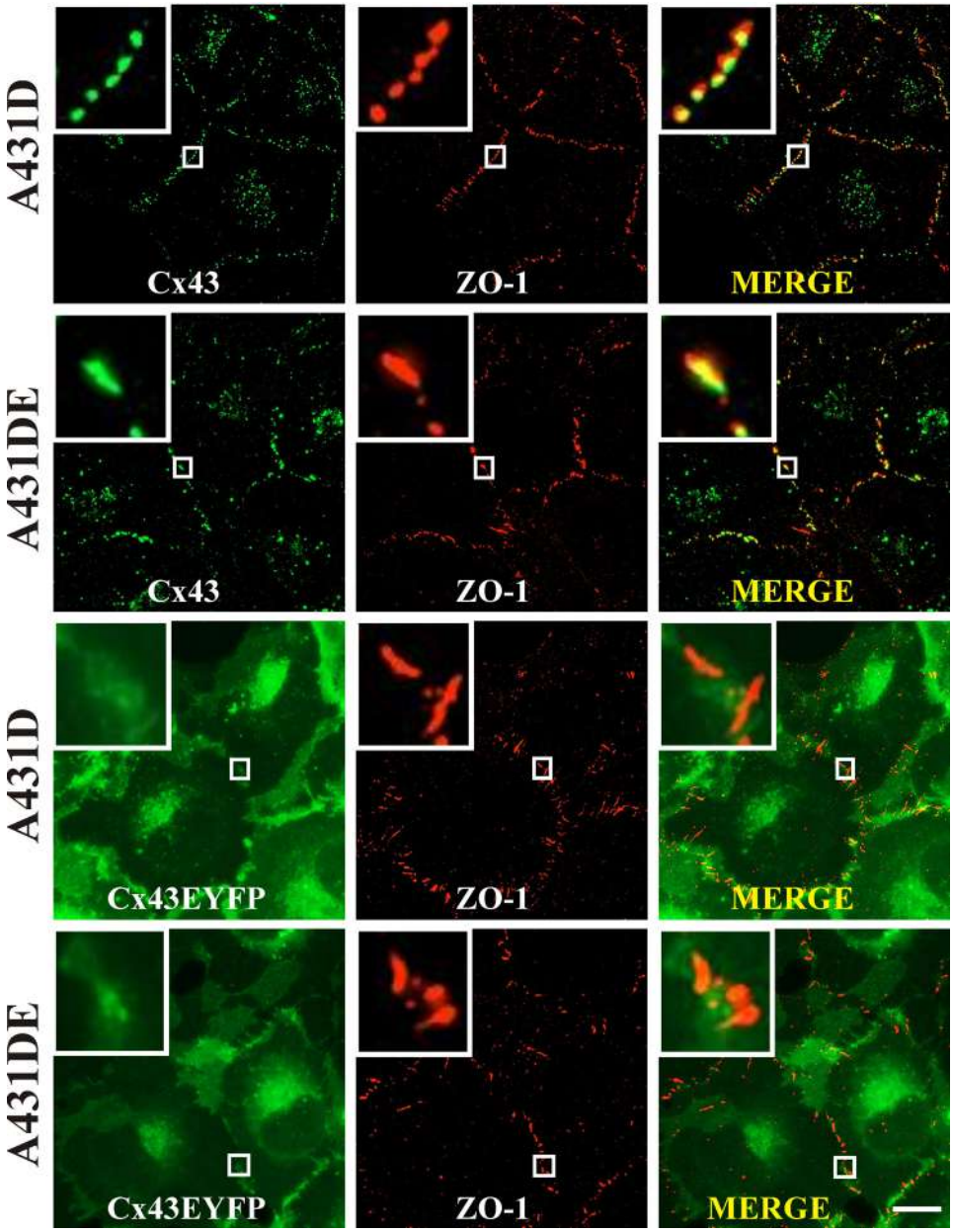

FIGURE 7. **Gap junction assembly-dependent co-localization of connexin43 and ZO-1.** Polyclonal cultures of A431D-43 and A431DE-43 cells, seeded on glass coverslips, were fixed, permeabilized, and immunostained for Cx43 (*green*) and ZO-1 (*red*), whereas those of Cx43-EYFP were immunostained for ZO-1 (see under "Materials and Methods"). The *insets* show the magnified images of co-localized Cx43 and ZO-1 puncta. Note that only untagged Cx43 is assembled into GJs and is co-localized with ZO-1. Note also that ZO-1 and Cx43-EYFP do not co-localize significantly. *Bar,* 10 μm.

A431DE-43 cells. First, we found that ZO-1 was localized as discrete puncta at cell-cell contact regions (Fig. 7, *top row, middle panels*). Second, ZO-1 co-localized extensively with untagged Cx43 (Fig. 7, *rows 1* and *2*) at the areas of cell-cell contact and not at intracellular sites. Third, as expected, ZO-1 did not co-localize with Cx43-EYFP (Fig. 7, *rows 3* and *4*) or with Cx43Δ257 and Cx43Δ363 (data not shown). Fourth, there was no noticeable difference in the pattern and the extent of co-localization of Cx43 and ZO-1 between A431D-43 and A431DE-43 cells.

Apart from binding to α-catenin, occludin, and claudins, ZO-1 has also been shown to bind actin (43, 44). Because Cx43 and ZO-1 co-localized extensively at the areas of cell-cell contact, and the fact that actin has been documented to play a critical role in the establishment and/maintenance of adherens and tight junctions (35, 45, 46), we examined the role of actin in GJ assembly. To test this notion, we immunostained Alexa Fluor 350-conjugated phalloidin-labeled A431D-43 and A431DE-43 cells for Cx43 and ZO-1 using Alexa Fluor 594- and Alexa Fluor 488-conjugated secondary antibodies. Fig. 8 shows that Cx43 and ZO-1 puncta appeared to associate with the actin fibers lining the cell peripheries.

To explore further the relationship between Cx43, ZO-1 and actin, we examined the effect of disrupting actin filaments on GJ assembly. Cells were treated with cytochalasin B (1 μg/ml) for 1–6 h, and the localization of F-actin, Cx43, and ZO-1 was examined as described above. Fig. 9 shows that in cadherin-null A431D-43 cells, cytochalasin B disrupted cortical F-actin and GJ puncta, which were displaced to subcellular compartments. These changes were observed as early as 1 h after treatment (Fig. 9, compare *rows 1* and *2*). On the other hand, in cadherin-expressing A431DE-43 cells, cytochalasin B failed to disrupt gap junctional plaques noticeably, and Cx43 and ZO-1 persisted as puncta at cell-cell contact areas (Fig. 9, compare *rows 3* and *4*) even up to 6 h (supplemental Fig. S11). Moreover, the depolymerization of actin itself appeared to have been delayed in A431DE-43 cells (supplemental Fig. S11). Also, we found that in cytochalasin B-treated A431D-43 cells, Cx43 and ZO-1 puncta appeared to co-localize in subcellular compartments, suggesting that they might have internalized together. Altogether, the above data suggest that intimacy between Cx43 and F-actin via ZO-1 may be required to maintain or stabilize GJ plaques. Moreover, the data also suggest that E-cadherin might facilitate the stabilization of gap junctional plaques via the direct or indirect interaction of plaque components with actin filaments.

ZO-1 Knockdown Attenuates Gap Junction Formation—To test directly if ZO-1 was required for the formation and/or maintenance of GJs, we silenced its expression by siRNAs in A431D-43 and A431DE-43 cells. For these experiments, we

Downloaded from www.jbc.org at Lehigh University, on November 10, 2010

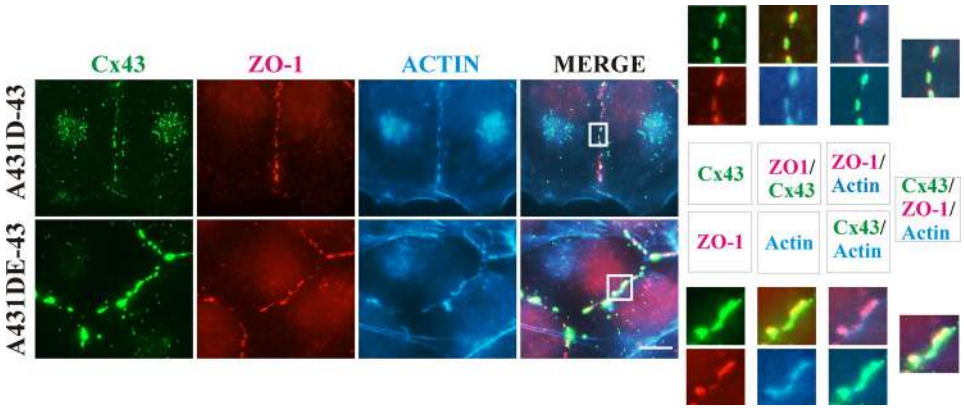

FIGURE 8. **Connexin43 and ZO-1 puncta are formed on F-actin at cell-cell contact.** A431D-43 (*top row*) and A431DE-43 (*bottom row*) cells, seeded on glass coverslips, were immunostained for Cx43 (*green*) and ZO-1 (*red*). F-actin (*blue*) was detected using Alexa Fluor 350-conjugated phalloidin. The magnified images of co-localized Cx43, ZO-1, and F-actin are shown on the *right*, and the key describing the corresponding images in color is shown in the *middle*. Note that significant co-localization of Cx43, ZO-1, and F-actin is observed only at puncta and at the regions of cell-cell contact. *Bar*, 5 μm.

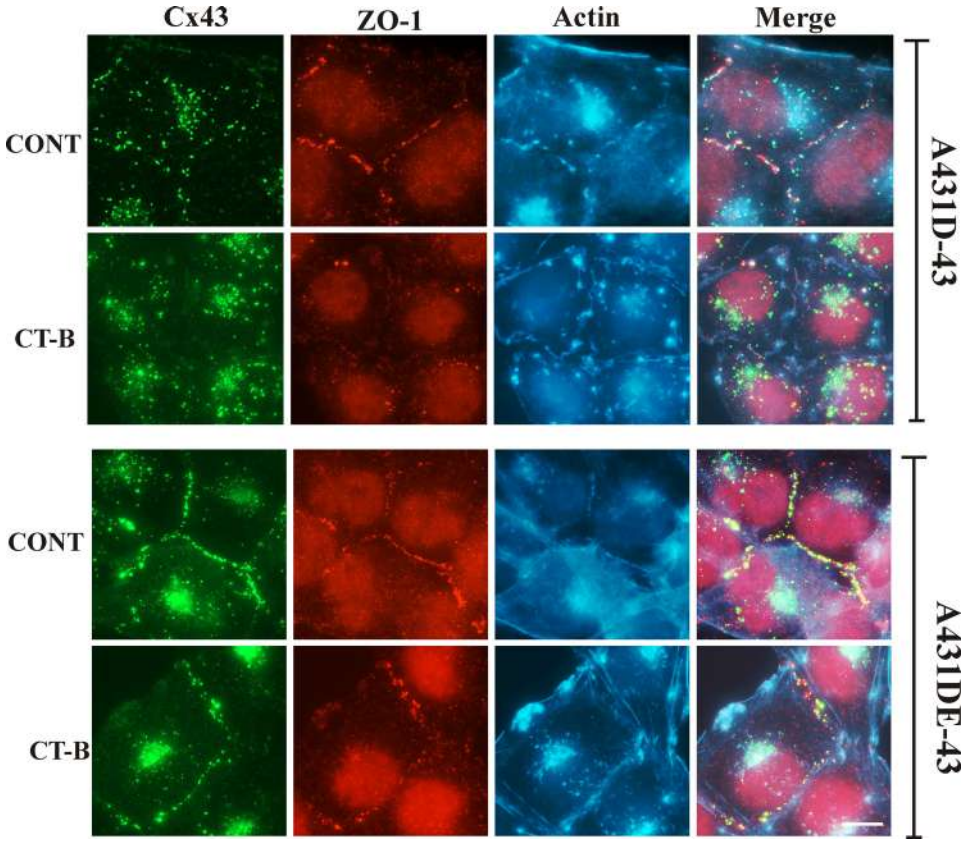

FIGURE 9. **E-cadherin delays gap junction disassembly.** A431D-43 and A431DE-43 cells, seeded on glass coverslips, were treated with cytochalasin B at 1 μg/ml (labeled *CT-B*) for 1–6 h and immunostained for Cx43 and ZO-1. F-actin was detected with Alexa Fluor 350-conjugated phalloidin. Note that co-localized GJ puncta of Cx43 and ZO-1 are disrupted/internalized within 1 h in A431D-43 cells, whereas no detectable disruption/internalization is noticed in A431DE-43 cells within 1 h and even until 6 h (supplemental Fig. S11). *Bar*, 5 μm. *CONT*, control.

used Dharmacon control siGLO and Smart Pool ZO-1 siRNAs. We first optimized experimental conditions, both duration and concentration of siRNAs, to achieve near 100% transfection efficiency in A431D-43 and A431DE-43 cells (supplemental Fig. S12*A*, and see "Materials and Methods"). As assessed by Western blot analysis of the total cell lysates, we consistently observed a robust 80–90% knockdown of ZO-1 (Fig. 10*A*). Immunocytochemical analysis showed that ZO-1 knockdown drastically diminished the preponderance of GJ puncta at the areas of cell-cell contact (Fig. 10*B*, *1st column*, compare *1st* and *2nd rows* with *3rd* and *4th rows*) and enhanced accumulation of Cx43 in the cytosol both in A431D-43 and A431DE-43 cells (Fig. 10*B*, *2nd* and *4th rows*, *right* and *left panels*). Knockdown of lamin A/C, a nuclear membrane-associated protein (data not shown), or mock transfection of control siRNAs (SiGLO) had no discernible effect on the formation of GJs (supplemental Fig. S12*B*). These findings suggest that ZO-1 is required to initiate and/or stabilize the formation of gap junctional plaques both in cadherin-null (A431D) and E-cadherin-expressing (A431DE) cells.

DISCUSSION

It is as yet unknown how the docking of connexons and the clustering of gap junctional channels are initiated upon cell-cell contact. Cadherins have been thought to facilitate the assembly of GJs by enhancing cell-cell contact; however, the molecular mechanisms involved in this process have remained unexplored. Here, we investigated whether E-cadherin expression was sufficient to facilitate the assembly of connexons into GJs via triggering cell-cell adhesion or whether additional events were required. To further explore the molecular mechanisms, we also examined the role of the carboxyl tail of Cx43, a ubiquitously expressed Cx (2, 18, 22), and of Cx32, a Cx expressed preferentially by the well differentiated and polarized cells (23), in controlling the formation of GJs in the presence and absence of E-cadherin. The rationale behind undertaking these studies was that the carboxyl termini of Cxs are highly divergent, are phosphorylated by several kinases, and interact with several proteins (21, 22), which might allow assembly to be regulated promiscuously by cadherins in a Cx-specific manner. For our studies, we utilized cadherin-null A431D cells, which have been used to examine adherens junc-

Downloaded from www.jbc.org at Lehigh University, on November 10, 2010

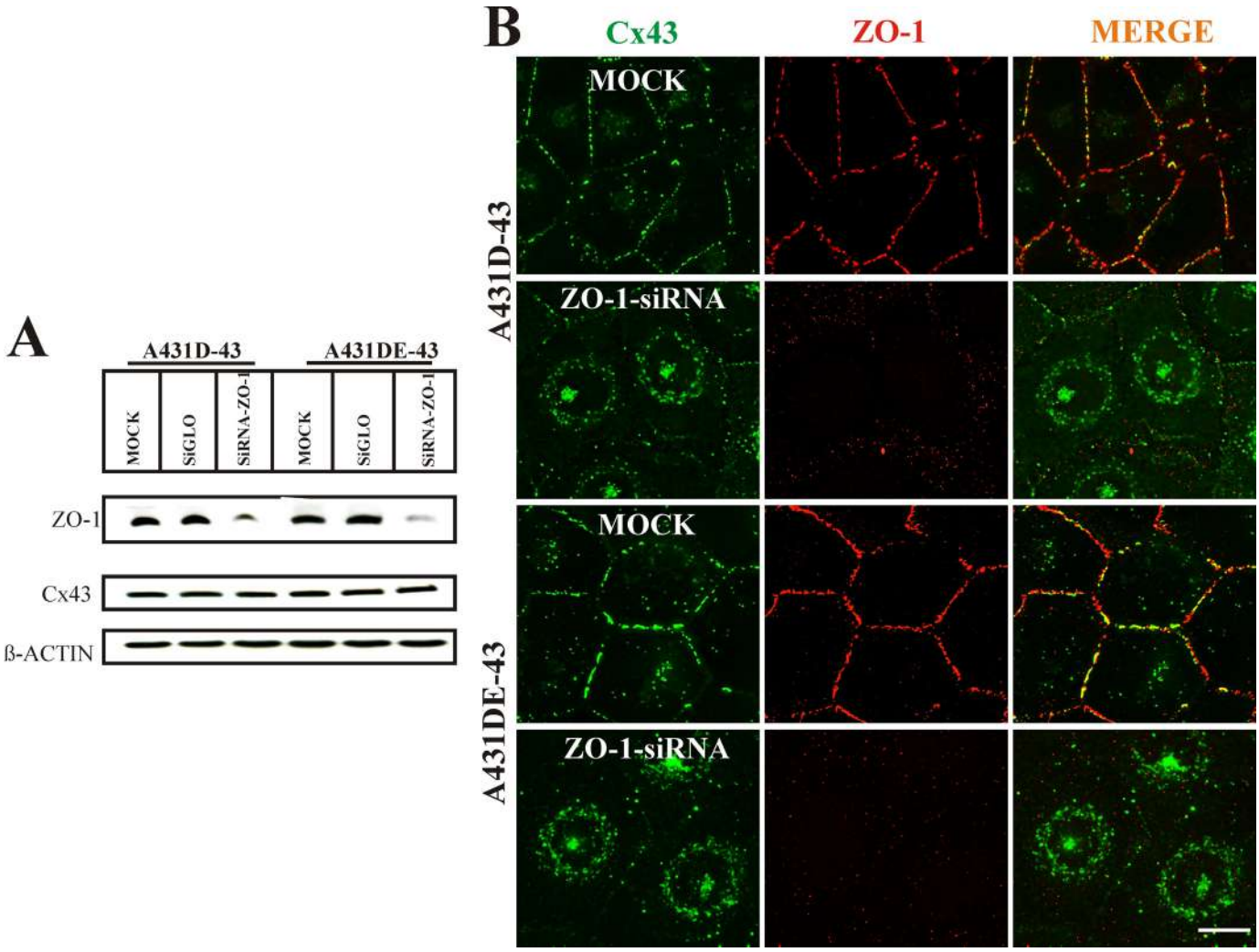

FIGURE 10. **ZO-1 knockdown disrupts gap junction assembly.** A431D-43 and A431DE-43 cells were either mock-transfected with Oligofectamine (labeled *MOCK*) or transfected with 130 nM ZO-1 SMARTpool siRNA (labeled *siRNA*) or DY-547-labeled control RISC-free siGLO RNA (labeled *SiGLO*) as described under "Materials and Methods." *A,* expression of ZO-1 and Cx43 was determined by immunoblotting 10 μg of total protein. The blots were re-probed with anti-β-actin antibody to verify equal loading. Note that ZO-1 expression is reduced significantly in cells transfected with ZO-1 SMARTpool siRNAs. *B,* cells were immunostained for Cx43 and ZO-1 together. Note that ZO-1 staining (*red*) is significantly reduced in ZO-1 SMART pool siRNA-transfected cells compared with MOCK-transfected cells. Note significant loss of gap junction puncta (*green*), with a concomitant increase in the intracellular Cx43 staining, in ZO-1 siRNA-transfected cells compared with MOCK-transfected cells. *Bar,* 10 μm.

Downloaded from www.jbc.org at Lehigh University, on November 10, 2010

tion assembly in previous studies (19, 20). Our findings documented that E-cadherin-mediated cell-cell adhesion was neither essential nor sufficient to initiate the formation of GJs *de novo* in A431D cells and facilitated the growth and assembly of only preformed GJs composed of Cx43. Growth of cells on Transwell filters was required to initiate the assembly of Cx32. Our findings also demonstrate a novel and an essential role of the carboxyl termini of Cx43 and Cx32 in initiating the formation of GJs *de novo* in A431D cells. Moreover, our studies further document that ZO-1 is required to initiate or stabilize GJs composed of Cx43 and that direct or indirect cross-talk between Cxs and the actin cytoskeleton via ZO-1 may be essential for GJ assembly.

Our biotinylation data showed that even though both Cxs trafficked normally to the cell surface (Fig. 3), only Cx43 was able to assemble into GJs (Fig. 1*A*). Moreover, E-cadherin expression facilitated the assembly of only Cx43 and failed to induce the assembly of Cx32 (Fig. 1*A*). These data suggest that the assembly of Cxs into GJs upon arrival at the cell surface is subject to regulatory mechanisms at the site of cell-cell contact that are likely to be Cx-specific and that cell-cell adhesion by itself is not sufficient to initiate the assembly. Because expression of Cx32 and Cx43 by itself neither triggered nor augmented E-cadherin-mediated cell-cell adhesion (supplemental Fig. S4), these regulatory mechanisms are likely to be cell-cell adhesion-independent, at least with regard to the type of adhesion measured by cell-cell aggregation assay, which has been widely used to document cell-cell adhesion mediated by cadherins (19, 32) as well as by Cxs (47, 48). Although previous studies have demonstrated an important role of cell-cell adhesion in facilitating GJ assembly (12–15), our findings do not rule out the causative role played by other cell-cell adhesion mechanisms that are independent of E-cadherin and connexins. Notwithstanding that such cell-cell adhesion systems likely exist in A431D cells, for example those mediated by nectins, NCAM, and JAMS, etc. (9, 10), they were insuffi-

cient to trigger the assembly of Cx32 in monolayer cultures, which suggests that the assembly was regulated promiscuously in a Cx-specific manner both in the presence and absence of E-cadherin.

With regard to the assembly of Cx43, E-cadherin expression not only increased the mean size of the GJs but also decreased the mean number of puncta per interface by 2-fold (supplemental Fig. S1 and Fig. S2). One plausible explanation for these data might be that formation of cadherin trans-dimers, or adherens junctions, initiates a signaling pathway that facilitates the coalescence of smaller puncta, which are highly dynamic and unstable (49, 50), into larger ones without affecting the frequency of plaque initiation, possibly via altering actin dynamics at the site of cell-cell contact (45). This explanation is in accord with the findings, which showed that expression of E-cadherin not only induced cell-cell adhesion in A431D cells (supplemental Fig. S4) but also stabilized expression and recruited α- and β-catenins to the site of cell-cell contact (Fig. 1, *B* and *D*). Moreover, this explanation is also in congruence with the findings that formation of cadherin trans-dimers appears to leave a distance of 20–25 nm between contiguous plasma membranes (10, 51), which is likely to hinder the docking of connexons that can protrude from the cell surface at the most by a few nanometers. Our findings with A431D cells showed that the assembly was triggered in the absence of measurable cell-cell adhesion, which had been presumed to be necessary.

Our data with cadherin-null A431D cells have unveiled a previously unrecognized essential role of the carboxyl tails of Cxs in initiating the assembly of GJs. In congruence with the findings reported in other studies, the carboxyl tail-deleted Cxs and the EYFP-tagged chimeras used in this study formed GJs in HEK293, HeLa, and the human prostate cancer cell line LNCaP. One possible explanation for these data is that in cadherin-null A431D cells, the linkage of Cxs to actin via carboxyl termini may be required to prime the initiation of GJ plaques before their maturation into larger plaques, as has been demonstrated during the genesis of adherens junctions (52–54), and that the requirement for this linkage is either bypassed or compensated by alternative pathway(s) used to assemble GJs when cadherins are present such as in N-cadherin-expressing HeLa and HEK293 cells and E-cadherin-expressing LNCaP cells (24, 55).

The carboxyl termini of Cxs interact with several proteins, such as ZO-1 and ZO-2, which are thought to form scaffolding complexes that link Cxs to the cytoskeleton (21, 22). Our findings showed that GJs were formed on actin-rich fibers at the areas of cell-cell contact where ZO-1 and Cx43 co-localized extensively (Fig. 8). Moreover, ZO-1 did not co-localize with Cx43-EYFP, Cx43Δ363, Cx43Δ257, and Cx43Δ257-EYFP, which failed to assemble into GJs in A431D cells (Fig. 7). Furthermore, GJs were disassembled within 1 h after cytochalasin B treatment in cadherin-null A431D43 cells, and the disassembly was delayed in E-cadherin-expressing A431DE-43 cells. Although the interaction of ZO-1 with Cx43 has been shown to modulate GJ assembly and disassembly, the mechanisms have not yet been elucidated. Our data imply that, at least in A431D and A431DE cells, a direct or indirect interaction between Cx43 and actin via ZO-1 may be required to initiate the formation of nascent GJ plaques or to stabilize them, and this interaction might be further strengthened by E-cadherin via α-catenin as has been observed during the formation of adherens junctions (52, 54). This explanation is in accord with our data, which showed that junctional plaques were more stable in E-cadherin-expressing A431DE-43 cells compared with cadherin-null A431D-43 cells. This notion is further substantiated by our data, which show that ZO-1 knockdown attenuated GJ assembly both in A431D-43 and A431DE-43 cells (Fig. 10), and by our findings demonstrating the failure of Cx43-EYFP, Cx43Δ363, Cx43Δ257, and Cx43Δ257-EYFP (which do not bind ZO-1) to assemble into GJs. This line of thought is further supported by the studies, which showed that the specific interaction between the PDZ2 domain of ZO-1 and Cx43 was required for GJ assembly but not for trafficking to the cell surface (56, 57). Our data also support the conclusions drawn from earlier studies, which showed that the clustering of cell-cell channels to form nascent GJ puncta and their incorporation into the plaques, but not the maintenance of matured GJ plaques, was dependent on an intact actin cytoskeleton (58–60).

The above arguments may also apply to the assembly of Cx32 into GJs in cells grown on Transwell filters. For example, Cx32 is predominantly expressed by well differentiated and polarized cells (23), and it is likely that its assembly into GJs might also be governed by the appropriate expression of proteins that maintain or are induced upon partial polarization and that allow it to interact with the cytoskeletal proteins via its carboxyl terminus. The acquisition of the polarized state is accompanied not only by extensive remodeling of cytoskeletal elements but also by recruitment of several protein complexes to the areas of cell-cell contact such as Crumbs complex and the partitioning defective complex (35, 46, 61–63). Connexin32, apart from interacting with caveolin-1 and Cx26, has been shown to interact with occludin, a tight junction-associated protein that binds ZO-1 (21), and with Discs Large Homolog-1 (64), a protein with multiple PDZ binding domains expressed in well differentiated and polarized cells. Moreover, this line of thought is consistent with the failure of carboxyl tail-deleted Cx32Δ220 and Cx32Δ220-EYFP to assemble into GJs in cadherin-null and E-cadherin-expressing cells (Fig. 6).

An intriguing aspect of the data with respect to the assembly of Cx32 on Transwell filters is that despite robust formation of GJ puncta and their detergent insolubility (Fig. 4), the channels did not permit the transfer of GJ-permeable fluorescent tracers, such as Lucifer Yellow, Alexa Fluor 488, and Alexa Fluor 594 (Table 2), which are known to pass through these channels (3). In this regard our data showed that when grown on Transwell filters for 3–6 days, A431D and A431DE cells, while becoming more columnar as assessed by a 2-fold increase in cell height compared with cells grown on plastic (supplemental Fig. S7), failed to attain a fully polarized state as assessed by the random orientation of Golgi stacks and distribution of β1-integrin, ZO-1, and Na-K-ATPase at the apical and basolateral domains (supplemental Fig. S7). Although there may be several explanations for these findings, one plausible explanation is that additional physiological stimuli or acquisition of a fully polarized state may be required to open these channels. Alternatively, GJs may serve yet another function independent of communication

Downloaded from www.jbc.org at Lehigh University, on November 10, 2010

when cells have acquired a polarized state, which is known to last from minutes to days or even years (46, 62, 63). The role of gap junctional communication in maintaining the polarized and the differentiated state of epithelial cells has not yet been investigated. Recent studies have shown that formation of GJs is required to induce the assembly of tight junctions or to maintain them (65). The fact that cell polarization also enhanced the assembly of Cx43 into gap junctions in cadherin-null A431D-43 cells, and E-cadherin expression had no further effect, suggests that its assembly might also be regulated by proteins that are induced upon polarization and that may allow maturation of gap junctional puncta in the absence of E-cadherin expression. Although the molecular mechanisms involved in the assembly of Cx32 into GJs in cells grown on Transwell filters remain to be investigated, our findings imply that distinct regulatory mechanisms are utilized to initiate its formation into nascent gap junctional plaques, the choice of which is likely dictated by the physiological state of the cells.

What might be the possible physiological relevance of E-cadherin-mediated facilitation of GJ assembly with regard to increase in plaque size, stability, and function of cell-cell channels? The number of channels in a given GJ plaque may range from 50 to over 10,000, and there is a wide range of variation in the size of GJs formed between two adjacent cells (3, 66). Moreover, clustering of cell-cell channels and increase in GJ size and function in response to polypeptide hormones is frequently observed (67). Furthermore, it has been demonstrated that clustering of cell-cell channels is a prerequisite for the opening of cell-cell channels and that larger GJ plaques have more open channels compared with smaller plaques in which most channels remain closed (68). Although our data showed that E-cadherin expression had no discernible effect on the permeability of fluorescent tracers, such as Lucifer Yellow, Alexa Fluor 488, and Alexa Fluor 594, it is possible that permeability to physiologically relevant molecules or to smaller molecules less than 443 Da was enhanced upon E-cadherin expression, which increases the frequency of larger GJ plaques in A431DE-43 cells. Alternatively, E-cadherin-mediated increase in GJ plaque size and stability may facilitate the assembly of other junctional complexes, which are required to maintain the polarized and differentiated state of epithelial cells (62, 63). More elaborate studies with a variety of cell-cell adhesion molecules are needed to assess further the physiological significance of our findings with respect to the functional role of gap junctional communication.

In essence, our studies with human A431D squamous carcinoma-derived cells have shown that the assembly of Cx43 and Cx32 upon arrival at the cell surface is regulated differently both in the absence and presence of E-cadherin, although the molecular nature of the mechanisms involved remains to be elaborated. We have also shown that E-cadherin-mediated cell-cell adhesion facilitates the assembly of GJs composed of Cx43 but is not sufficient to induce the assembly of Cx32. Using A431D and A431DE cells, we have uncovered a role for the carboxyl tails of Cx43 and Cx32 in initiating the *de novo* formation of GJs, which had remained previously unrecognized. Our data also imply that direct or indirect cross-talk between carboxyl tails of Cxs and actin cytoskeleton via ZO-1 may regulate GJ assembly and growth. The fact that our findings pertaining to the role of E-cadherin and ZO-1 in regulating the assembly of Cxs into GJs in A431D cell culture model systems are different from those reported in other cell culture models implies that multiple regulatory mechanisms are likely utilized in a physiological state, cell context, and internal and external milieu-dependent manner to control GJ size, dynamics, and growth. Future studies will be needed to fully understand and elaborate the molecular mechanism by which E-cadherin expression facilitates the assembly of Cx43 into GJs, how cross-talk between Cx43 and actin via ZO-1 regulates plaque dynamics and assembly, and how cell growth on Transwell filters facilitates the assembly of Cx32 into GJs.

Acknowledgments—We thank Kristen Johnson, Linda Kelsey, and Parul Katoch for technical help and friendship.

REFERENCES

1. Beyer, E. C., and Berthoud, V. M. (2009) in *Connexins: A Guide* (Harris, A., and Locke, D., eds) pp. 3–26, Springer, Humana Press, NY
2. Laird, D. W. (2006) *Biochem. J.* **394,** 527–543
3. Sosinsky, G. E., and Nicholson, B. J. (2005) *Biochim. Biophys. Acta* **1711,** 99–125
4. Falk, M. M., Baker, S. M., Gumpert, A. M., Segretain, D., and Buckheit, R. W., 3rd (2009) *Mol. Biol. Cell* **20,** 3342–3352
5. Gaietta, G., Deerinck, T. J., Adams, S. R., Bouwer, J., Tour, O., Laird, D. W., Sosinsky, G. E., Tsien, R. Y., and Ellisman, M. H. (2002) *Science* **296,** 503–507
6. Jordan, K., Chodock, R., Hand, A. R., and Laird, D. W. (2001) *J. Cell Sci.* **114,** 763–773
7. Piehl, M., Lehmann, C., Gumpert, A., Denizot, J. P., Segretain, D., and Falk, M. M. (2007) *Mol. Biol. Cell* **18,** 337–347
8. Musil, L. S. (2009) in *Connexins: A Guide* (Harris, A., and Locke, D., eds) pp. 225–240, Springer, Humana Press, NY
9. Nelson, W. J. (2008) *Biochem. Soc. Trans.* **36,** 149–155
10. Tepass, U., Trunong, K., Godt, D., Ikura, M., and Peifer, M. (2000) *Nat. Rev. Cell Mol. Biol.* **1,** 91–100
11. Wheelock, M. J., and Johnson, K. R. (2003) *Annu. Rev. Cell Dev. Biol.* **19,** 207–235
12. Hernandez-Blazquez, F. J., Joazeiro, P. P., Omori, Y., and Yamasaki, H. (2001) *Exp. Cell Res.* **270,** 235–247
13. Jongen, W. M., Fitzgerald, D. J., Asamoto, M., Piccoli, C., Slaga, T. J., Gros, D., Takeichi, M., and Yamasaki, H. (1991) *J. Cell Biol.* **114,** 545–555
14. Meyer, R. A., Laird, D. W., Revel, J. P., and Johnson, R. G. (1992) *J. Cell Biol.* **119,** 179–189
15. Musil, L. S., Cunningham, B. A., Edelman, G. M., and Goodenough, D. A. (1990) *J. Cell Biol.* **111,** 2077–2088
16. Crespin, S., Defamie, N., Cronier, L., and Mesnil, M. (2009) in *Connexins: A Guide* (Harris, A., and Locke, D., eds) pp. 529–542, Springer, Humana Press, NY
17. Thiery, J. P., and Sleeman, J. P. (2006) *Nat. Rev. Mol. Cell Biol.* **7,** 131–142
18. Wei, C. J., Xu, X., and Lo, C. W. (2004) *Annu. Rev. Cell Dev. Biol.* **20,** 811–838
19. Lewis, J. E., Wahl, J. K., 3rd, Sass, K. M., Jensen, P. J., Johnson, K. R., and Wheelock, M. J. (1997) *J. Cell Biol.* **136,** 919–934
20. Sobolik-Delmaire, T., Katafiasz, D., and Wahl, J. K., 3rd (2006) *J. Biol. Chem.* **281,** 16962–16970
21. Hervé, J. C., Bourmeyster, N., Sarrouilhe, D., and Duffy, H. S. (2007) *Prog. Biophys. Mol. Biol.* **94,** 29–65
22. Solan, J. L., and Lampe, P. D. (2009) *Biochem. J.* **419,** 261–272
23. Bavamian, S., Klee, P., Allagnat, F., Haefliger, J. A., and Meda, P. (2009) in *Connexins: A Guide* (Harris, A., and Locke, D., eds) pp. 511–527, Springer,

Downloaded from www.jbc.org at Lehigh University, on November 10, 2010

Humana Press, NY
24. Mitra, S., Annamalai, L., Chakraborty, S., Johnson, K., Song, X. H., Batra, S. K., and Mehta, P. P. (2006) *Mol. Biol. Cell* **17,** 5400–5416
25. Govindarajan, R., Zhao, S., Song, X. H., Guo, R. J., Wheelock, M., Johnson, K. R., and Mehta, P. P. (2002) *J. Biol. Chem.* **277,** 50087–50097
26. Mehta, P. P., Perez-Stable, C., Nadji, M., Mian, M., Asotra, K., and Roos, B. A. (1999) *Dev. Genet.* **24,** 91–110
27. Lauf, U., Lopez, P., and Falk, M. M. (2001) *FEBS Lett.* **498,** 11–15
28. VanSlyke, J. K., and Musil, L. S. (2000) *Methods* **20,** 156–164
29. Shintani, Y., Fukumoto, Y., Chaika, N., Svoboda, R., Wheelock, M. J., and Johnson, K. R. (2008) *J. Cell Biol.* **180,** 1277–1289
30. Rudnicki, J. A., and McBurney, M. W. (1987) in *Teratocarcinomas and Embryonic Stem Cells: A Practical Approach* (Robertson, E. J., ed) pp. 19–49, IRL Press at Oxford University Press, Oxford
31. Gourdie, R. G., Green, C. R., and Severs, N. J. (1991) *J. Cell Sci.* **99,** 41–55
32. Kim, S. H., Li, Z., and Sacks, D. B. (2000) *J. Biol. Chem.* **275,** 36999–37005
33. Mills, I. G., Jones, A. T., and Clague, M. J. (1998) *Curr. Biol.* **8,** 881–884
34. Nakamura, N., Rabouille, C., Watson, R., Nilsson, T., Hui, N., Slusarewicz, P., Kreis, T. E., and Warren, G. (1995) *J. Cell Biol.* **131,** 1715–1726
35. Rodriguez-Boulan, E., Kreitzer, G., and Müsch, A. (2005) *Nat. Rev. Mol. Cell Biol.* **6,** 233–247
36. Solan, J. L., and Lampe, P. D. (2009) in *Connexins: A Guide* (Harris, A., and Locke, D., eds) pp. 263–286, Springer, Humana Press, NY
37. Hunter, A. W., Barker, R. J., Zhu, C., and Gourdie, R. G. (2005) *Mol. Biol. Cell* **16,** 5686–5698
38. Giepmans, B. N., Verlaan, I., Hengeveld, T., Janssen, H., Calafat, J., Falk, M. M., and Moolenaar, W. H. (2001) *Curr. Biol.* **11,** 1364–1368
39. Giepmans, B. N., and Moolenaar, W. H. (1998) *Curr. Biol.* **8,** 931–934
40. Elfgang, C., Eckert, R., Lichtenberg-Fraté, H., Butterweck, A., Traub, O., Klein, R. A., Hülser, D. F., and Willecke, K. (1995) *J. Cell Biol.* **129,** 805–817
41. Lauf, U., Giepmans, B. N., Lopez, P., Braconnot, S., Chen, S. C., and Falk, M. M. (2002) *Proc. Natl. Acad. Sci. U.S.A.* **99,** 10446–10451
42. Giepmans, B. N., Hengeveld, T., Postma, F. R., and Moolenaar, W. H. (2001) *J. Biol. Chem.* **276,** 8544–8549
43. Fanning, A. S., Jameson, B. J., Jesaitis, L. A., and Anderson, J. M. (1998) *J. Biol. Chem.* **273,** 29745–29753
44. Fanning, A. S., Ma, T. Y., and Anderson, J. M. (2002) *FASEB J.* **16,** 1835–1837
45. Mège, R. M., Gavard, J., and Lambert, M. (2006) *Curr. Opin. Cell Biol.* **18,** 541–548
46. Li, R., and Gundersen, G. G. (2008) *Nat. Rev. Mol. Cell Biol.* **9,** 860–873
47. Cotrina, M. L., Lin, J. H., and Nedergaard, M. (2008) *Glia* **56,** 1791–1798
48. Lin, J. H., Takano, T., Cotrina, M. L., Arcuino, G., Kang, J., Liu, S., Gao, Q., Jiang, L., Li, F., Lichtenberg-Frate, H., Haubrich, S., Willecke, K., Goldman, S. A., and Nedergaard, M. (2002) *J. Neurosci.* **22,** 4302–4311
49. Holm, I., Mikhailov, A., Jillson, T., and Rose, B. (1999) *Eur. J. Cell Biol.* **78,** 856–866
50. Jordan, K., Solan, J. L., Dominguez, M., Sia, M., Hand, A., Lampe, P. D., and Laird, D. W. (1999) *Mol. Biol. Cell* **10,** 2033–2050
51. Miyaguchi, K. (2000) *J. Struct. Biol.* **132,** 169–178
52. Adams, C. L., Chen, Y. T., Smith, S. J., and Nelson, W. J. (1998) *J. Cell Biol.* **142,** 1105–1119
53. Itoh, M., Nagafuchi, A., Moroi, S., and Tsukita, S. (1997) *J. Cell Biol.* **138,** 181–192
54. Vasioukhin, V., Bauer, C., Yin, M., and Fuchs, E. (2000) *Cell* **100,** 209–219
55. Shaw, R. M., Fay, A. J., Puthenveedu, M. A., von Zastrow, M., Jan, Y. N., and Jan, L. Y. (2007) *Cell* **128,** 547–560
56. Chen, J., Pan, L., Wei, Z., Zhao, Y., and Zhang, M. (2008) *EMBO J.* **27,** 2113–2123
57. Hunter, A. W., and Gourdie, R. G. (2008) *Cell Commun. Adhes.* **15,** 55–63
58. Johnson, R. G., Meyer, R. A., Li, X. R., Preus, D. M., Tan, L., Grunenwald, H., Paulson, A. F., Laird, D. W., and Sheridan, J. D. (2002) *Exp. Cell Res.* **275,** 67–80
59. Thomas, T., Jordan, K., and Laird, D. W. (2001) *Cell Commun. Adhes.* **8,** 231–236
60. Wang, Y., and Rose, B. (1995) *J. Cell Sci.* **108,** 3501–3508
61. Bornens, M. (2008) *Nat. Rev. Mol. Cell Biol.* **9,** 874–886
62. Bryant, D. M., and Mostov, K. E. (2008) *Nat. Rev. Mol. Cell Biol.* **9,** 887–901
63. Mellman, I., and Nelson, W. J. (2008) *Nat. Rev. Mol. Cell Biol.* **9,** 833–845
64. Duffy, H. S., Iacobas, I., Hotchkiss, K., Hirst-Jensen, B. J., Bosco, A., Dandachi, N., Dermietzel, R., Sorgen, P. L., and Spray, D. C. (2007) *J. Biol. Chem.* **282,** 9789–9796
65. Kojima, T., Murata, M., Go, M., Spray, D. C., and Sawada, N. (2007) *J. Membr. Biol.* **217,** 13–19
66. Sosinsky, G. E., Gaietta, G., and Giepmans, B. N. (2009) in *Connexins: A Guide* (Harris, A., and Locke, D., eds) pp. 241–261, Springer, Humana Press, NY
67. Stagg, R. B., and Fletcher, W. H. (1990) *Endocr. Rev.* **11,** 302–325
68. Bukauskas, F. F., Jordan, K., Bukauskiene, A., Bennett, M. V., Lampe, P. D., Laird, D. W., and Verselis, V. K. (2000) *Proc. Natl. Acad. Sci. U.S.A.* **97,** 2556–2561
69. Deleted in proof

Downloaded from www.jbc.org at Lehigh University, on November 10, 2010

Supplementary Figures

Figure S-1 (A) E-cadherin expression increases the size of gap junctions composed of connexin43. A431D-43 and A431DE-43 cells, seeded on glass cover slips, were extracted with 1% Triton X-100 *in situ* and immunostained for Cx43. Area and the length of 120 distinct GJ puncta were determined using the measurement module of Volocity from single optical sections after iterative volume deconvolution of the captured images. The area is represented as pixels whereas length is represented in relative units (see Materials and Methods). Note the higher frequency of longer and larger GJ plaques in E-cadherin expressing A431DE-43 cells. Average GJ area and length from the data obtained for GJ area and length distribution analyses were calculated and plotted. Note the two fold increase in the average GJ plaque area and length upon E-cadherin expression. The differences in area and length between A431D-43 and A431DE-43 cells were statistically highly significant ($P \leq 0.001$).

Figure S-2. E-cadherin expression decreases number of gap junctions per cell-cell interface. A431D-43 and A431DE-43 cells were extracted with 1 % TX-100 *in situ* and immunostained as described for Figure S-1. Images were captured using 0.5µm Z-steps and deconvolved. The number of GJ puncta per cell-cell interface was determined after merging all the deconvolved image stacks into a single plane (see Materials and Methods). Between sixty and seventy such cell-cell interfaces of deconvolved image stacks from three independent experiments were used and the mean number of GJ puncta per cell-cell interface was then calculated and plotted. Note that the number of GJ puncta per cell-cell interface decreased two-fold in A431DE-43 cells as compared with A431D-43 cells. The difference in mean number of puncta per cell-cell interface between A431D-43 and A431DE-43 cells was statistically highly significant ($P \leq 0.001$).

Figure S-3. Connexin43 is phosphorylated in A431D-43 and A431D-43 cells like other cells that form gap junctions. Total cell lysates were prepared from A431D-43 and A431DE-43 cells and other normal and transformed cancer cell lines that differ widely in their ability to assemble Cx43 into GJs. **A.** The lysates were probed with the following anti-Cx43 antibodies: 1. Rabbit polyclonal antibody raised against peptide containing amino acid residues 362-382 of Cx43 (Sigma, Cat # 6219). 2. Rabbit polyclonal antibody raised against residues 252-271 (69). 3. Rabbit polyclonal antibody (Cell signaling, Cat # 3512). 4. Rabbit polyclonal antibody which detects Cx43 phosphorylated at Ser 368 (Cell Signaling, Cat # 3511). 5. Mouse monoclonal antibody raised against residues 252-270 (BD Transduction Laboratories; Cat # 610062). 6. Mouse monoclonal antibody raised against peptide containing amino acid residues 362-381of Cx43 (Sigma Cat # 8093). 7. Mouse monoclonal antibody which detects Cx43 when it is not phosphorylated at ser 368 (Invitrogen; Cat # 13-8300). **B**. Various Cx43 expressing cell lines were immunostained for Cx43 using rabbit polyclonal antibody raised against peptide containing amino acid residues 362-382 of Cx43 (Sigma, Cat # 6219). 1. LNCaP43-1 and LNCaP43-2: Two sub-clones derived from human prostate cancer cell line after retroviral transduction of Cx43 (26). 2. HEK293 cells that express Cx43 endogenously. 3. Human pancreatic cancer cell line, BxPC3, which expresses endogenous Cx43 and fails to form gap junctions. 4. RL-CL9-12, a sub-clone derived

Downloaded from www.jbc.org at Lehigh University, on November 10, 2010

from rat liver clone 9 (RL-CL-9) cells, which forms gap junctions (69), and RL-CL9-11, a sub-clone derived from RL-CL-9 cells, which fails to form GJs.

Figure S-4. Connexin expression neither induces nor affects E-cadherin-mediated cell-cell adhesion. A. Five thousand cells (A431D-32, A431D-43, A431DE-32 and A431DE-43), suspended in a 20 µl of complete medium and placed on the lids of petri dishes, were allowed to aggregate. Images were captured following overnight incubation (see Methods). Note that E-cadherin expressing cells (A431DE, A431DE-32, and A431DE-43; bottom row) form aggregates compared to cadherin-null A431D cells (A431D, A431D-32 and A431D-43 clones; see top row). Also note that the size of aggregates formed in A431DE cells is independent of the subtype of Cx expressed. **B**. The size of aggregates from four random snapshots obtained from two independent experiments was measured and the average aggregate size was calculated and plotted as described (see Methods). The bars represent the standard error of the mean. As assessed visually, in cadherin null cells only a few aggregates of loosely bound cells are formed whereas aggregates formed of E-cadherin-expressing cells are large and more compact. Note that connexin expression does not affect the size of the aggregates. The differences in the mean sizes of the aggregates among A431D, A431D-43 and A431D-32 as well as among A431DE, A431DE-43 and A431DE-32 cells were not statistically significant ($P \geq 0.8$**).** The difference between the mean size of the aggregates between A431D and A431DE was statistically significant ($P \leq 0.001$).

Figure S-5. Gap junctional communication in parental and connexin expressing A431D and A431DE cells. Parental and Cx32 or Cx43 expressing A431D and A431DE cells were microinjected with the fluorescent tracer, Alexa-488 (MW 570), and the junctional transfer was determined (see Materials and Methods). Note extensive junctional transfer in Cx43-expressing A431D-43 and A431DE-43 cells. Note also lack of junctional transfer in parental and A431D-32 and A431DE-32 cells. The microinjected cells are marked by the arrows. Similar data were obtained when cells were microinjected with Lucifer Yellow and Alexa Fluor 594 (See Table 1 and 2).

Figure S-6. Co-localization of connexins in A431D and A431DE cells grown on trans-well filters. Cadherin null A431D-32 and A431D-43 and E-cadherin expressing A431DE-32 and A431DE-43 cells, seeded on glass cover slips, were immunostained for Cx32 or Cx43 (green) and GM-130 (red). Note that both Cx43 and Cx32 co-localize with GM-130. The boxed region is magnified and shown in the inset. Bar = 15 µm.

Figure S-7. Partial apical-basolateral polarization of A431D and A431DE grown on trans-well filters. A. Cadherin null A431D-32 and A431D-43 and E-cadherin expressing A431DE-32 and A431DE-43 cells, seeded on trans-well filters and glass cover slips in parallel, were grown for 5 days and immunostained for Cx32 or Cx43 (green) and ZO-1 (red). The serial *z* -sections (0.5 µm) were collected and analyzed with image-processing software Volocity (see Methods). The XZ cross-sectional images were computer generated using Volocity software. The apical surfaces of the cells are at the top edge while the basal surfaces at the bottom edge in each panel. Note that ZO-1 is localized at the baso-lateral as well as sub-apical surface in cells grown on trans-well filters as compared with those grown on cover slips. Note basolateral

Downloaded from www.jbc.org at Lehigh University, on November 10, 2010

localization of Cx43 and Cx32 in cells grown on trans-well filters and cover slips. Also note columnar organization of cells grown on trans-well filters as compared with those grown on glass cover slips, as assessed by the height of the cells, which has increased considerably in cells grown on filters. **B**. A431D and A431DE cells grown on trans-well filters for 5 days were immunostained for β1-integrin, NaK-ATPase, and GM130 (red). The nuclei were stained with DAPI (blue). The XZ cross-sectional images generated as described (see Materials and Methods). The apical surface of the cell is at the top edge while the basal surface at the bottom edge in each panel. Note similar distribution of β1-integrin (basal and intracellular), NaK-ATPase (at the lateral surface), and GM130 (localized mainly at one side of the nucleus) in A431D and A431DE cells grown on filters and on glass-cover slips. Bar = 10 μm.

Figure S-8. Growth on trans-well filters augments the assembly of connexin43. A. A431D-32 and A431DE-32 cells were grown on glass cover slips for five days in parallel experiments to those shown in Figure 4. Note failure of Cx32 to form GJs. **B, C.** A431D-43 and A431DE-43 cells were grown on either filters **(B)** or glass cover slips (C) for 5 days and extracted in situ with 1 % TX-100 (see Methods). Note that Cx43 is assembled into bigger GJs in A431D-43 and A431DE-43 cells grown on filters and there appears to be no significant difference in the size and abundance of GJs between cover slip- and filter-grown A431DE-43 cells. Bar = 10 μm.

Figure S-9. Carboxyl terminally tagged Cx43-EYFP chimeras fail to assemble into gap junctions on trans well filters. Polyclonal cultures of A431D and A431DE cells expressing Cx43Δ257-EYFP and Cx43-EYFP and Cx43Δ233-EYFP (not shown) were grown for six days on trans-well filters and extracted *in situ* with 1 % Triton-X-100 (see Methods). Cells were observed under immunofluorescence microscope following fixation. Note diffuse intracellular localization of all EYFP-tagged Cx43 chimeras and their failure to assemble into discrete puncta. Note also their disappearance upon *in situ* extraction. Bar = 20 μm.

Figure S-10. Sub-cellular fate of connexin43-EYFP chimeras in HeLa and LNCaP cells. A. Cx43Δ233-EYFP, Cx43Δ257EYFP, and Cx43-EYFP were introduced into HeLa (top row) and LNCaP cells (bottom row) using recombinant retroviruses (see Materials and Methods). The cells were fixed and observed after 24 h. Note that while chimeras Cx43-EYFP and Cx43Δ257-EYFP formed large GJs, chimera Cx43Δ233-EYFP remained scattered throughout the cytoplasm and failed to form GJs. (C,D) HeLa cells, seeded in 6 cm dishes, were transfected with 6 μg of pEYFP, pCx43Δ233-EYFP, pCx43Δ257-EYFP, pCx43-EYFP, and Cx43 (C), and with pCx32-EYFP and pCx32Δ220-EYFP (D) as described in Materials and Methods. After 24-36 h the cells were lysed and 10 μg of total protein was immunoblotted using anti-GFP (EYFP, Cx43Δ233-EYFP, Cx43Δ257-EYFP, and Cx43-EYFP), anti-Cx43 antibodies (for untagged Cx43) and anti-Cx32 antibody for tagged and untagged Cx32 chimeras. The immunoblots show that all the chimeras are expressed and migrate at positions corresponding to their expected molecular weights.

Figure S-11. E-cadherin delays gap junction disassembly. A431D-43 (top) and A431DE-43 (bottom) cells, seeded on glass cover slips, were treated with

Downloaded from www.jbc.org at Lehigh University, on November 10, 2010

cytochalasin B (CT-B) at 1μg/ml for 1-6 h and immunostained for Cx43 (green) and ZO-1 (red). F-actin was detected with Alexa-350-conjugated phalloidin. Note that no detectable disruption/ internalization of co-localized GJ puncta is noticed in A431DE-43 cells even up to 6 h whereas the puncta are disrupted/internalized within 1 h in A431D-43 (See also Figure 8 legend).

Figure S-12. A. Transfection efficiency of RNA oligonucleotides in A431D and A431DE cells. A431D-43 and A431DE-43 cells were transfected with 130 nM DY-547-labeled control RISC-free siGLO RNAs (red) as described in the Methods. After 72 h, cells were fixed and stained with DAPI to label the nuclei (Blue). Note near 100 % transfection efficiency. **B. Transfection of control RISC-free siGLO RNA does not affect gap junction assembly.** Cells were transfected with control siRNA and immunostained for Cx43 and ZO-1 together. Note that ZO-1 staining (red) is not significantly affected. Note also lack of significant effect on gap junctions (green) at the cell-cell contact areas.

Downloaded from www.jbc.org at Lehigh University, on November 10, 2010

Figure S-1

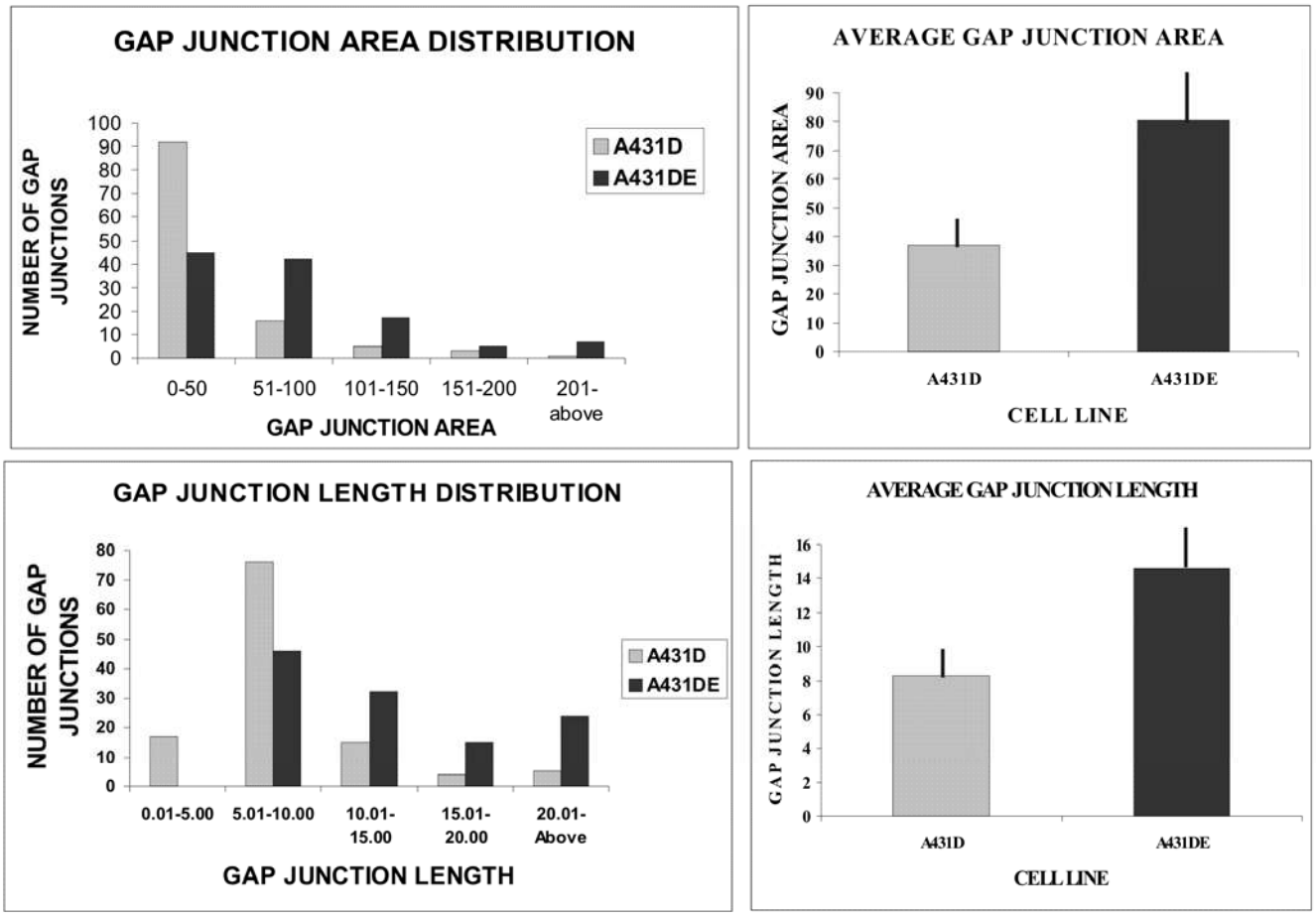

Downloaded from www.jbc.org at Lehigh University, on November 10, 2010

Figure S-2

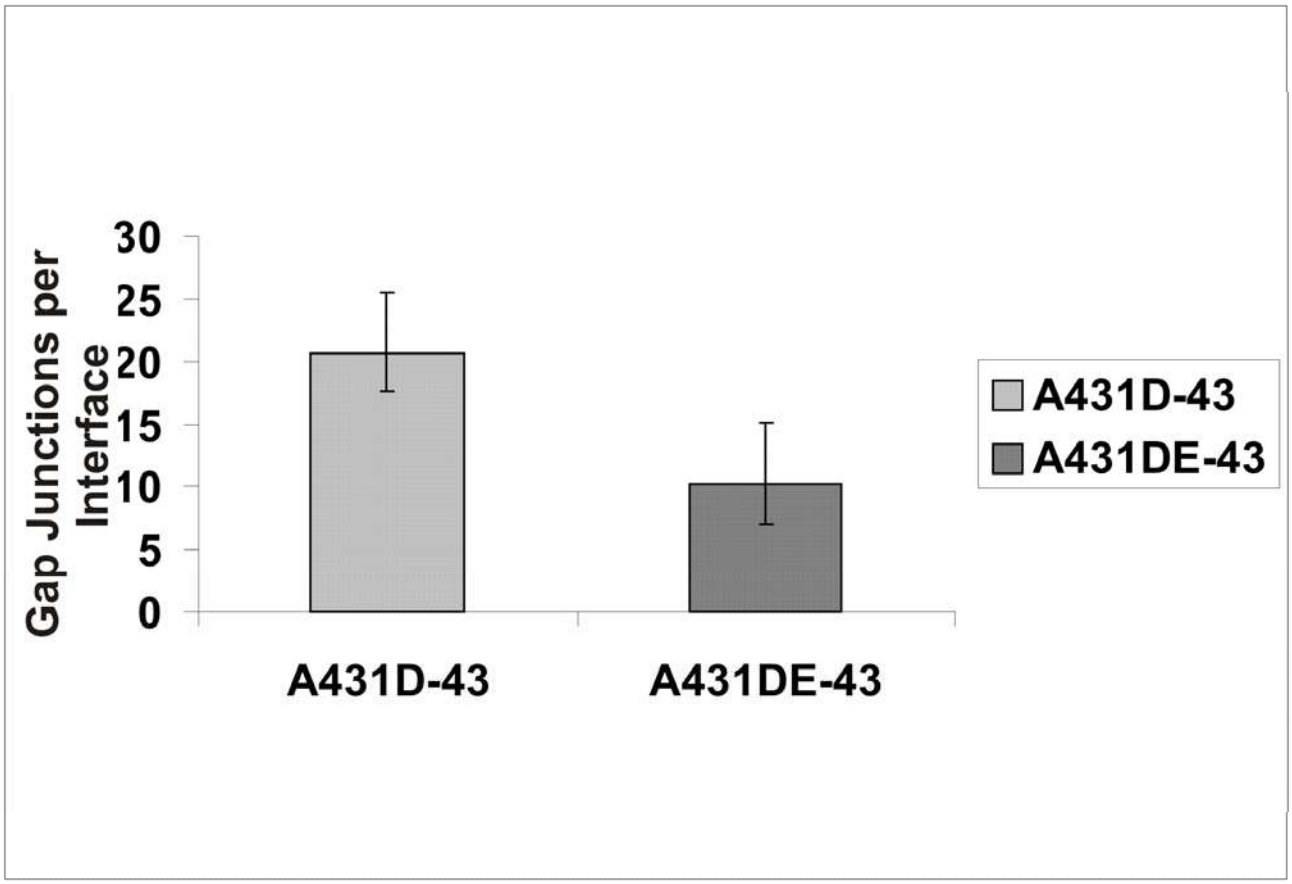

Downloaded from www.jbc.org at Lehigh University, on November 10, 2010

Figure S-3

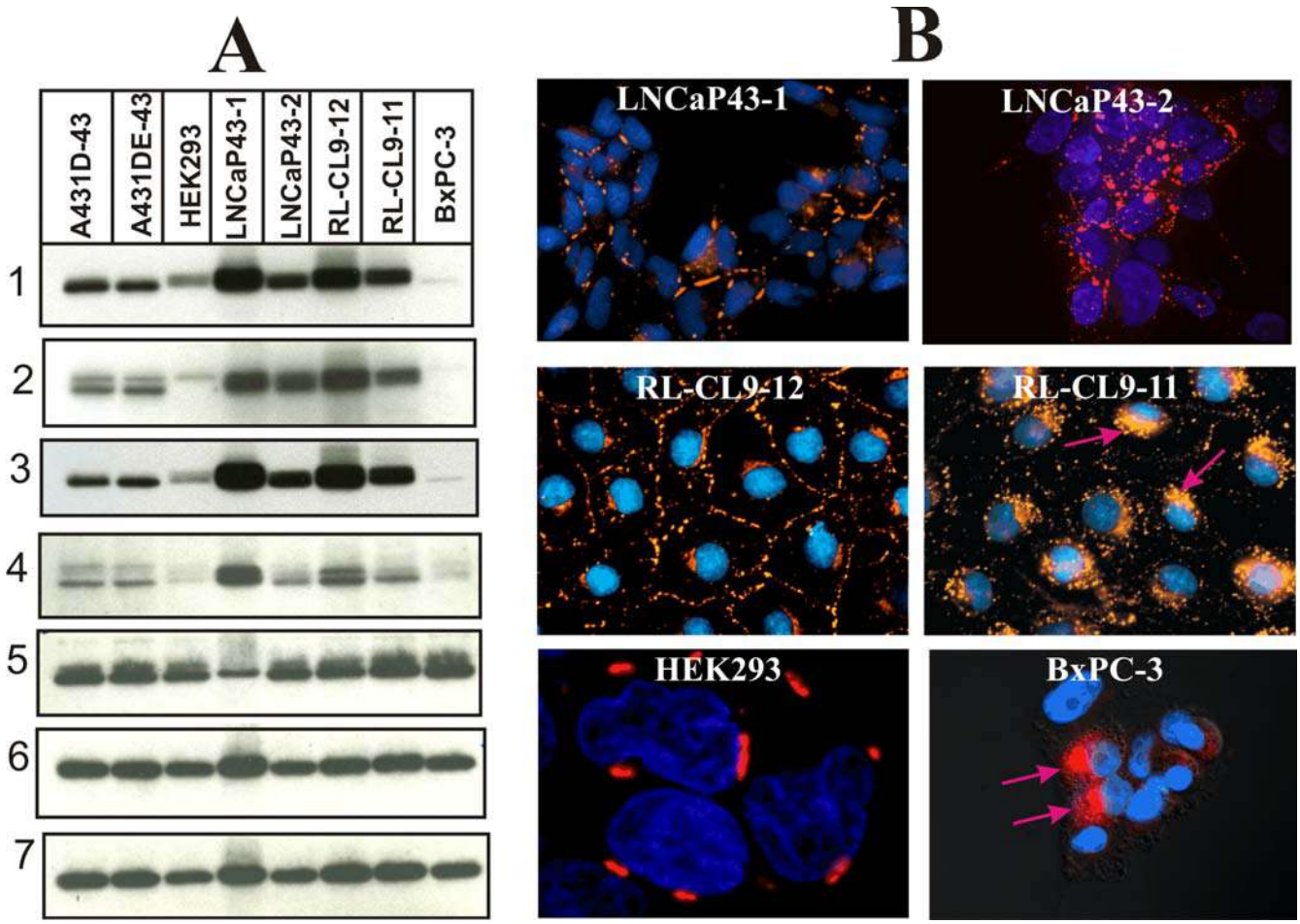

Downloaded from www.jbc.org at Lehigh University, on November 10, 2010

Figure S-4

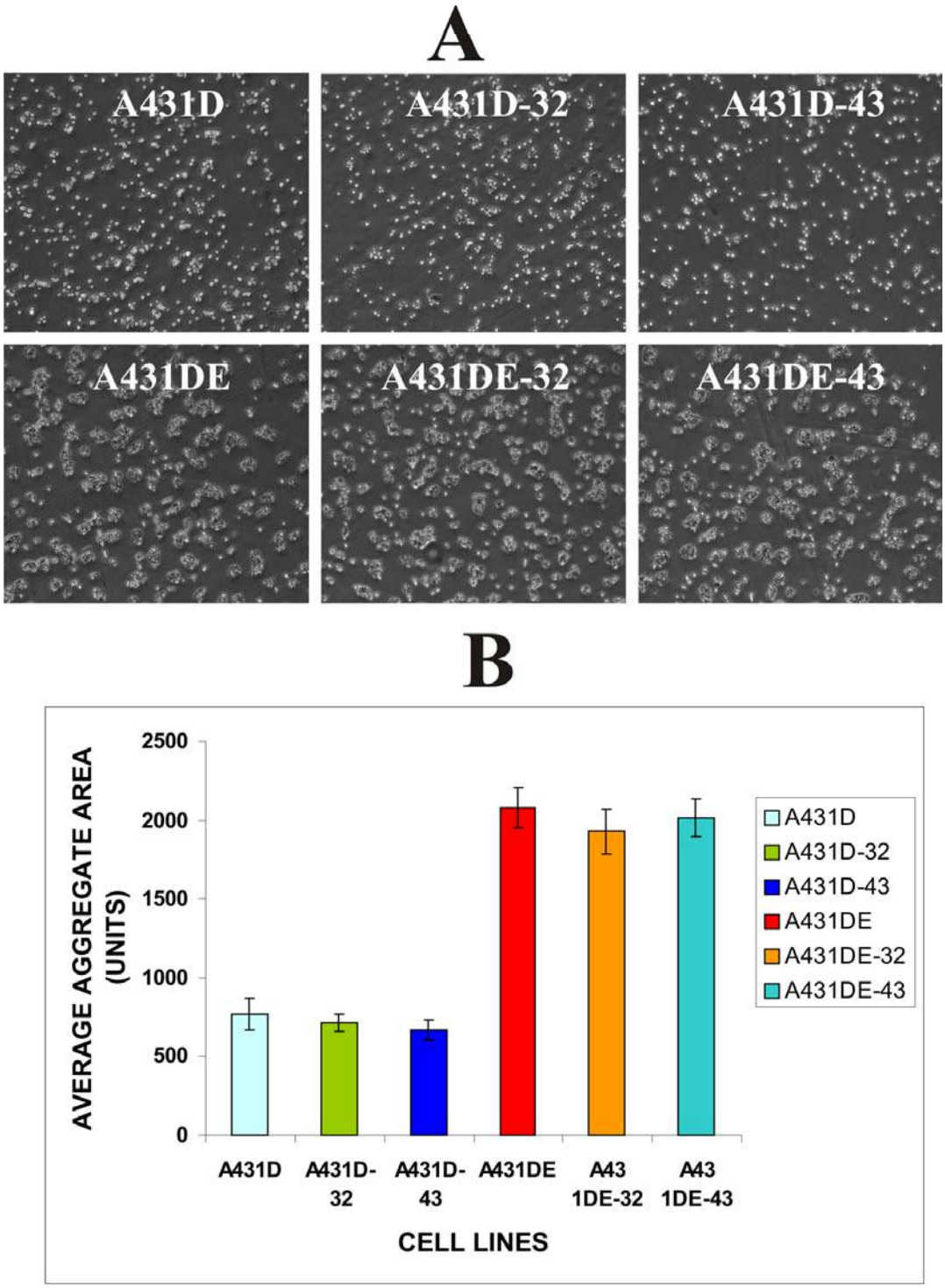

Downloaded from www.jbc.org at Lehigh University, on November 10, 2010

Figure S-5

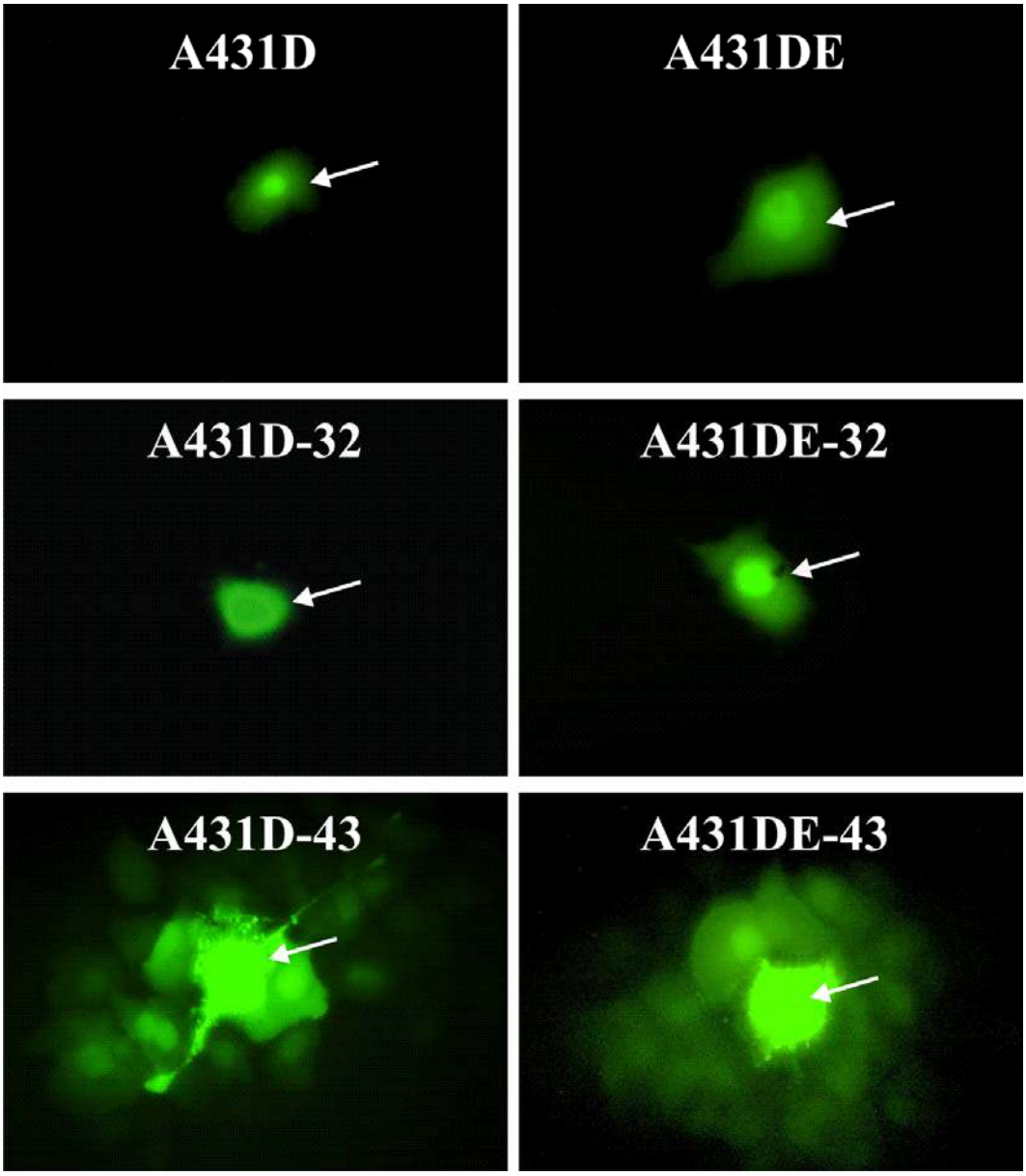

Downloaded from www.jbc.org at Lehigh University, on November 10, 2010

Figure S-6

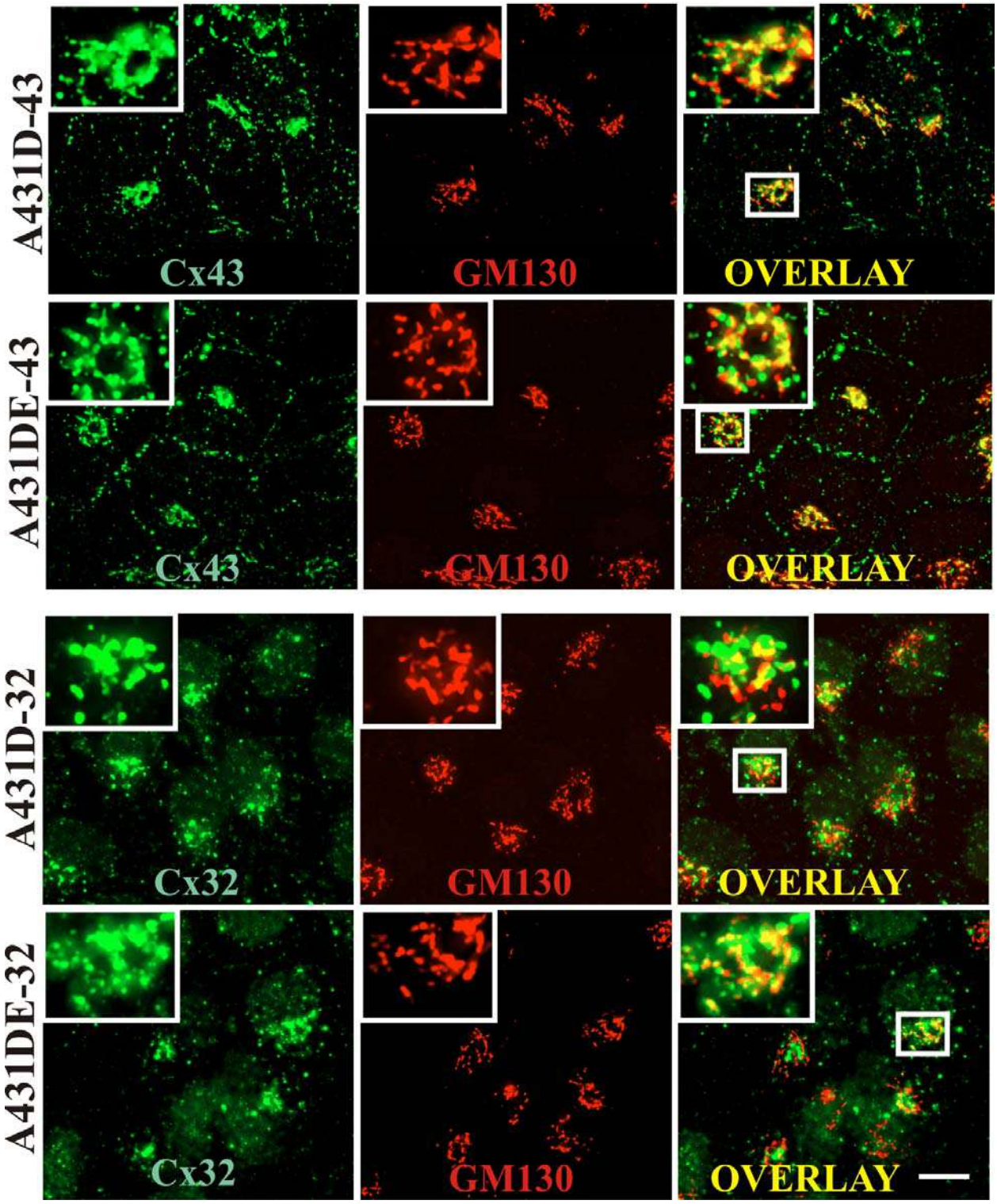

Downloaded from www.jbc.org at Lehigh University, on November 10, 2010

Figure S-7

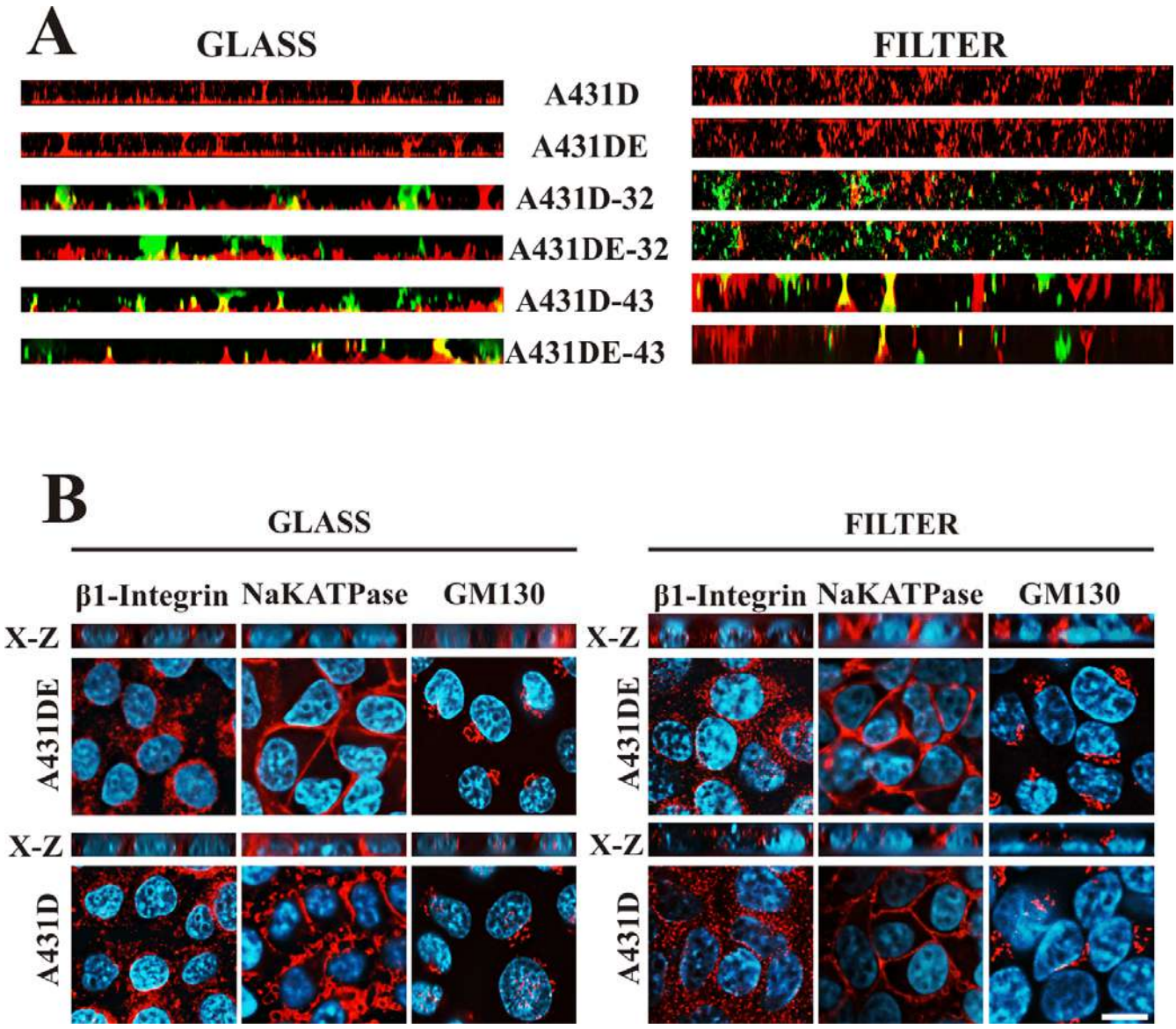

Downloaded from www.jbc.org at Lehigh University, on November 10, 2010

Figure S-8

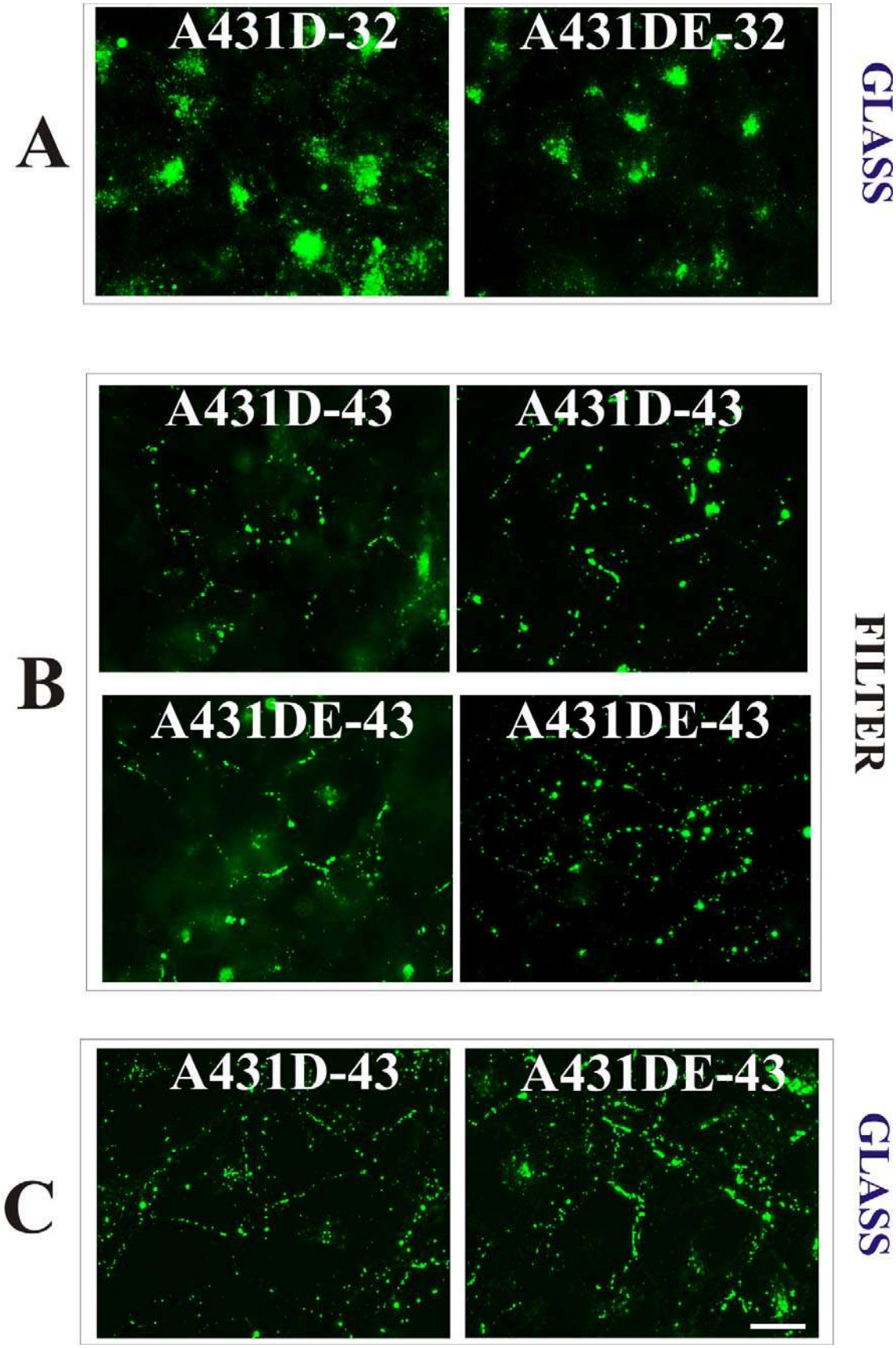

Downloaded from www.jbc.org at Lehigh University, on November 10, 2010

Figure S-9

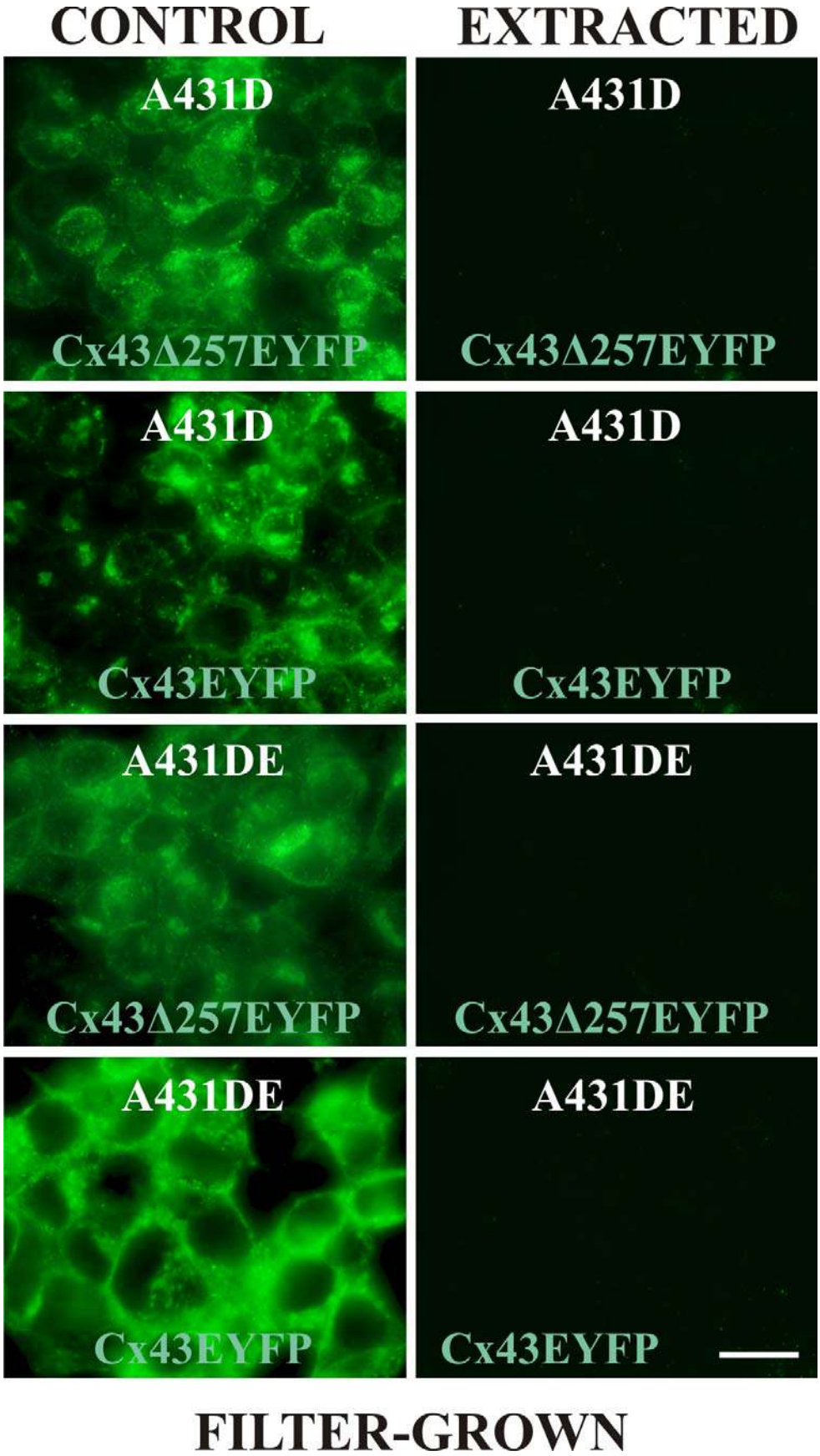

Downloaded from www.jbc.org at Lehigh University, on November 10, 2010

Figure S-10

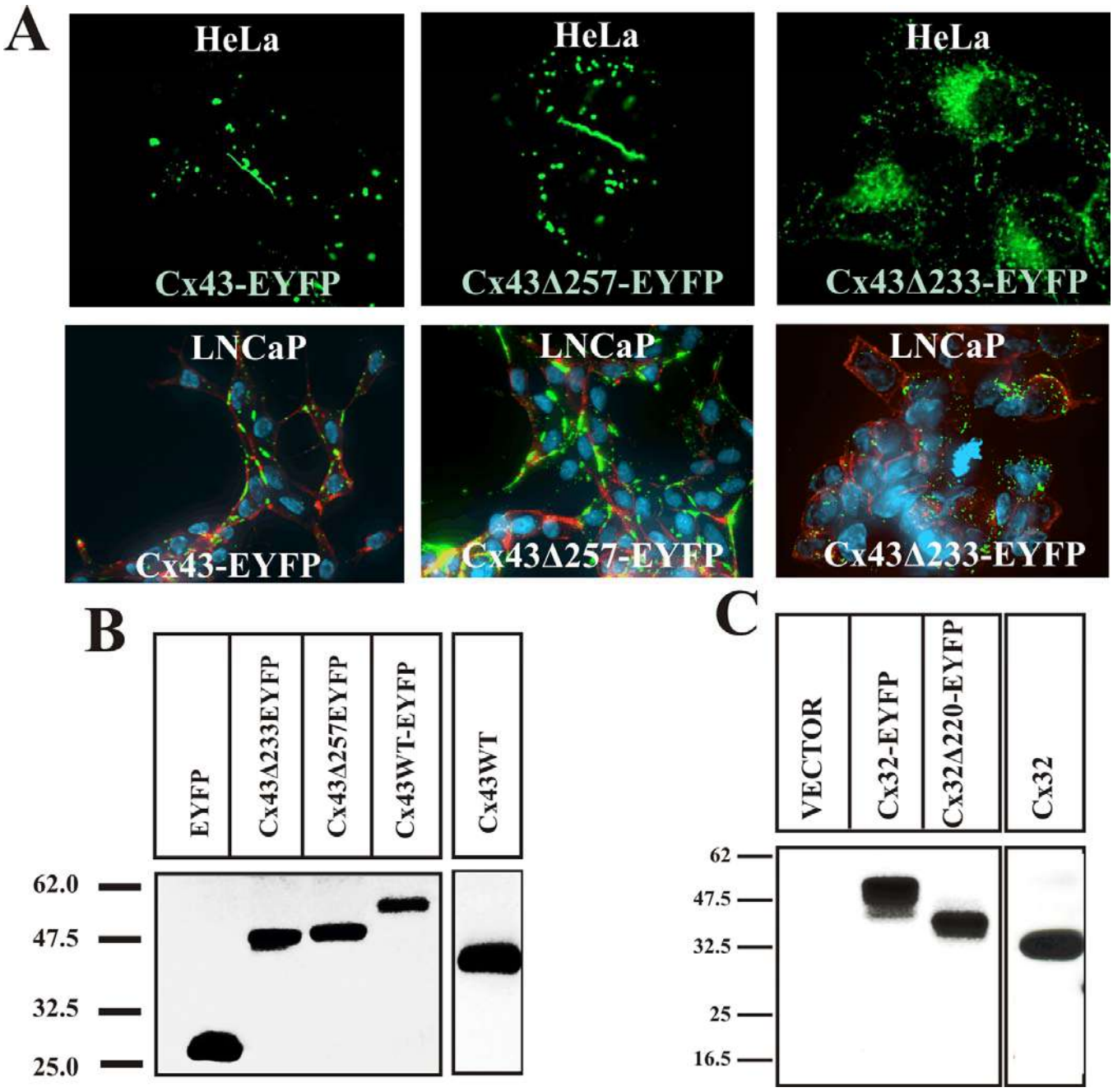

Downloaded from www.jbc.org at Lehigh University, on November 10, 2010

Figure S-11

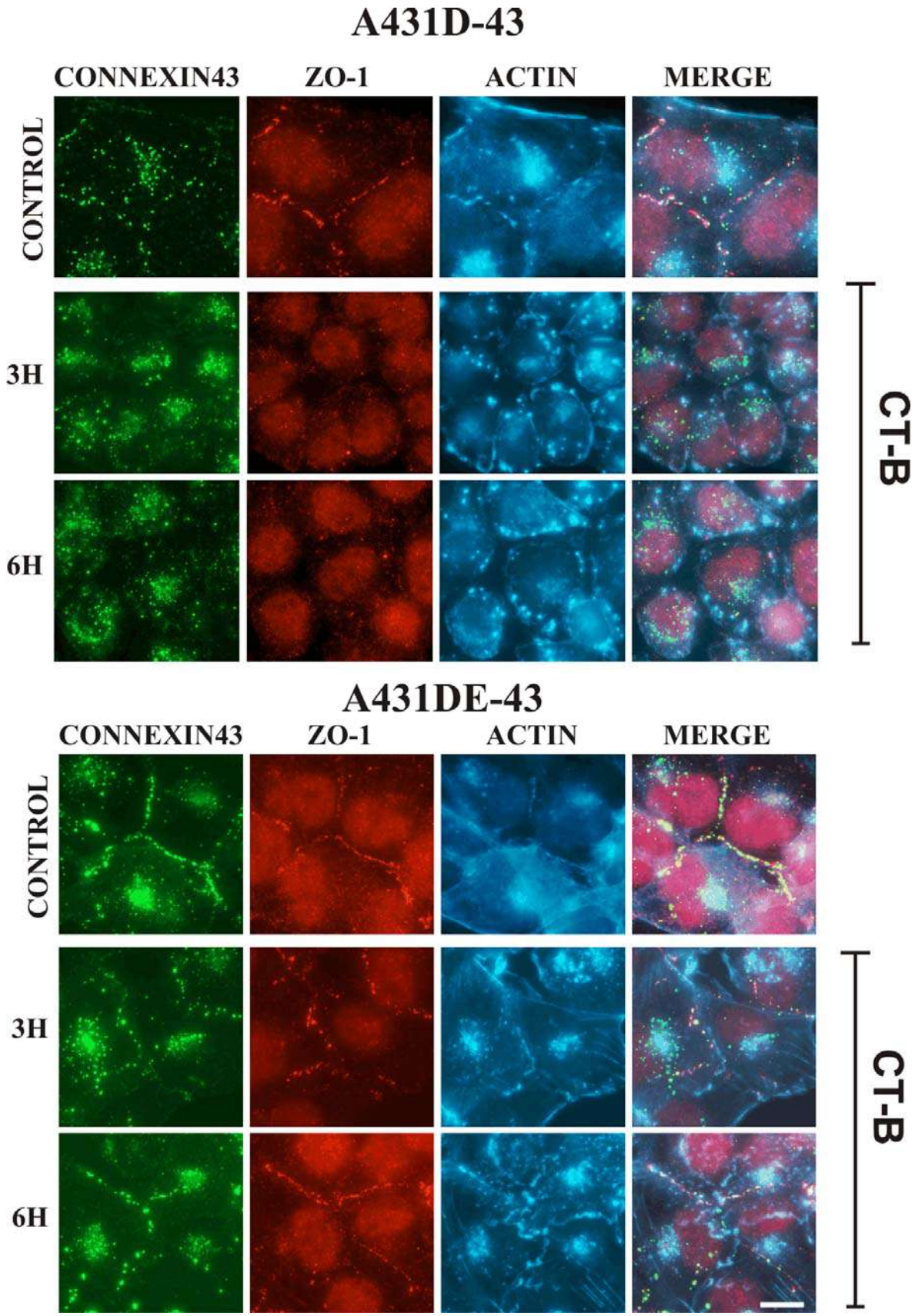

Downloaded from www.jbc.org at Lehigh University, on November 10, 2010

Figure S-12

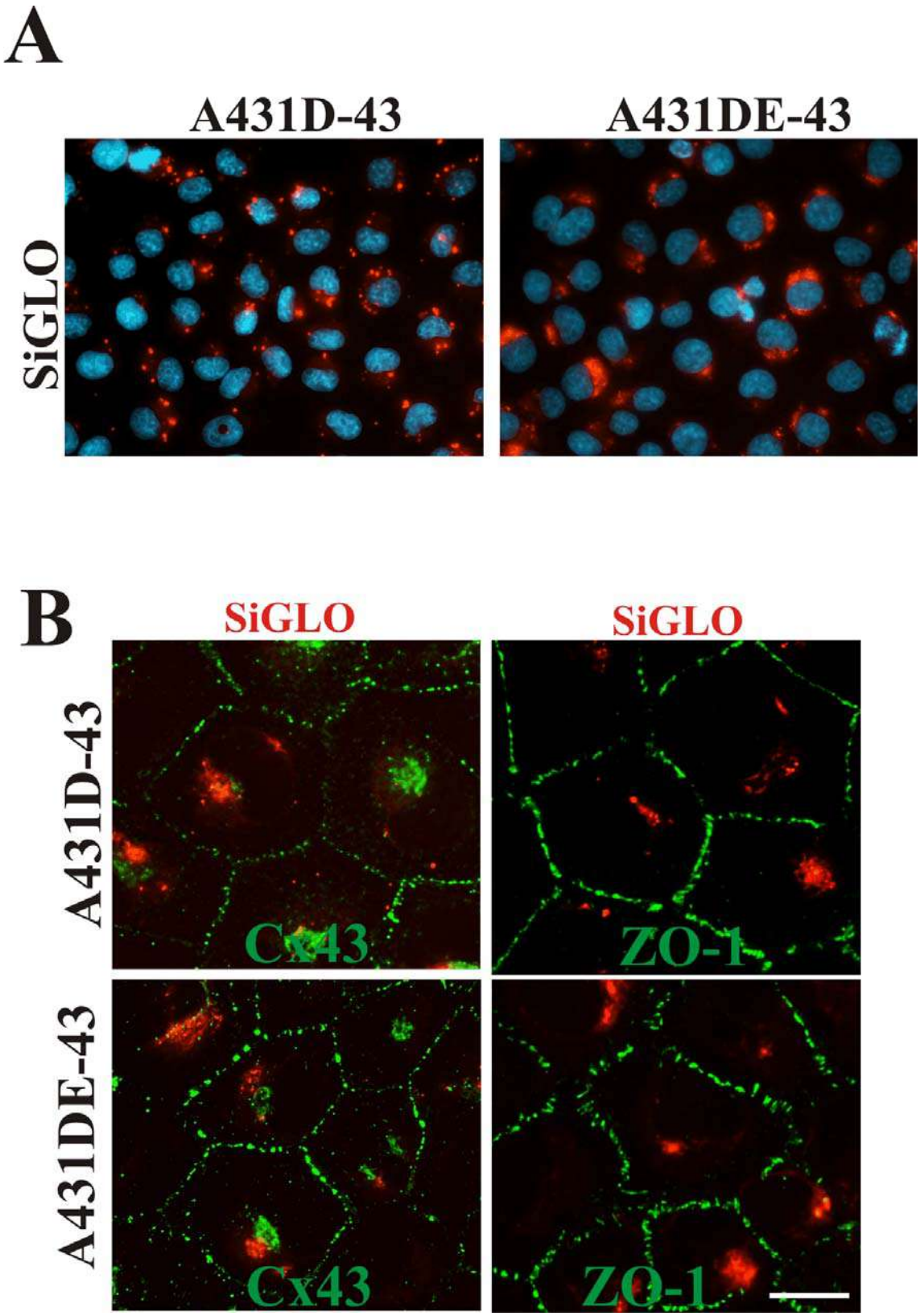

Downloaded from www.jbc.org at Lehigh University, on November 10, 2010